WORKING PAPERS

N° 1746

May 2026

"The Stranding Cost of Agricultural Subsidies under Climate-Transition and Biodiversity-Regulation Risks"

Manh-Hung Nguyen

Toulouse School of Economics

The Stranding Cost of Agricultural Subsidies under Climate-Transition and Biodiversity-Regulation Risks*

Manh-Hung Nguyen†

May 12, 2026

Abstract

Anticipated carbon pricing and biodiversity regulation turn agricultural subsidies into stranded assets. In a continuous-time model of partially irreversible capital under Poisson policy arrival, calibrated to Danish dairy, the stranding loss is strictly convex in the capital overhang. Under full pass-through of CAP support into livestock capital, Common Agricultural Policy payments amplify the loss by a factor of 13.2; at a 25% pass-through the multiplier is 1.7. A second biodiversity risk contracts the capital target by 60 percent; expected stranding losses are supermodular in the subsidy pair in the risk-neutral benchmark and satisfy the same ranking numerically in the calibrated HJB, so joint reform dominates staged reform. The welfare-maximising subsidy is zero once the social cost of methane exceeds €19/tCO_2e.

JEL Codes: E22, H23, Q18, Q54, Q57

Keywords: irreversible investment, policy risk, stranded assets, carbon taxation, biodiversity regulation, subsidy design

*I thank Toan Phan and Mathias Reynaert for valuable comments and participants at the IREEDS seminar for helpful discussions. The author acknowledges funding from the French National Research Agency (ANR) under the Investment for the Future (Investissements d'Avenir) program, grant ANR-17-EURE-0010.

†Toulouse School of Economics, INRAE, Université de Toulouse Capitole, Toulouse, France. E-mail: manh-hung.nguyen@tse-fr.eu.

1 Introduction

Climate policy revalues capital that is already in the ground. The mechanism is climate *transition* risk: the repricing of long-lived capital under anticipated regulation, distinct from the physical impacts of warming itself (Campiglio et al., 2023; Phan, 2026). A Danish dairy farmer operating under Common Agricultural Policy (CAP) payments has invested in herd, parlour, barn housing, and slurry storage — assets priced against the pre-regulation user cost. A future carbon tax renders part of that stock redundant. Livestock clears only at meat value; specialised equipment trades in thin secondary markets; decommissioning takes time. Anticipating reform, the farmer adjusts today, but only imperfectly: convex costs block rapid disinvestment, and resale recovers a fraction of replacement cost. How much of the resulting stranding loss is endogenous to the subsidy that financed the accumulation?

The stakes are high. The 2021–2027 CAP commits about €56 billion per year — roughly €42 billion in direct payments and €14 billion in rural development, including insurance-premium subsidies (European Commission, 2024). Agriculture accounts for about 10 percent of EU greenhouse-gas emissions, three-quarters of which come from livestock through enteric methane and manure management (European Environment Agency, 2024).

The Green Deal targets a 55 percent reduction by 2030. In 2024 Denmark adopted the Green Tripartite agreement, which phases in an agricultural emissions tax from 2030, with headline rates rising from DKK 300/tCO_2e to DKK 750/tCO_2e by 2035 and a 60 percent base deduction (Danish Ministry of Taxation, 2024). Biodiversity policy is moving in parallel: the EU Nature Restoration Regulation, adopted in 2024, imposes legally binding ecosystem-restoration targets that bear directly on livestock production on biodiversity-sensitive land (European Union, 2024). Animal-sourced-food assets represent 78 percent of fixed agricultural capital in the EU27 and face stranding exposure of 18–77 percent under plausible dietary-shift and carbon-pricing scenarios (Kortleve et al., 2025). Other member states are weighing comparable measures.

Subsidies inflate the capital stock above the level that will be optimal once a tax arrives. Partial irreversibility blocks costless unwinding at reform, and the resulting welfare loss grows faster than linearly in the gap between inherited and post-reform capital. Subsidy-induced accumulation therefore compounds in welfare rather than accruing linearly. A second policy risk, biodiversity regulation, operates on the same margin.

Under the full-pass-through benchmark, the subsidy raises the pre-regulation herd from 49 to 207 livestock units, while the post-regulation target is only 21 LU, so K^*/K_∞ is close to ten. The welfare loss at reform is 13.2 times the loss without the subsidy, decomposing as 6.6 in the static accounting comparator, 8.7 in the structural frictionless benchmark, and 13.2 in the dynamic model with convex adjustment.

Risk aversion and the subsidy are complements. At the calibrated $\gamma = 2$, the consumption-gap channel raises K^* by roughly 8% above the risk-neutral baseline; the increase rises to 15–25% across $\gamma \in [1, 4]$ and rises with the subsidy.

The policy margin identifies a threshold for reform. The welfare-maximising subsidy is zero

once the social cost of methane exceeds about €19 per tonne of CO_2-equivalent. This threshold lies below standard methane damage valuations under GWP_{100} conversion and is close to the corresponding GWP_{20} value. Agricultural-insurance subsidies — 70 percent of crop-insurance premiums in France, 62 to 80 percent in the United States — operate on the same margin, and joint reform strictly dominates the sequential alternative. A second biodiversity risk — peatland restoration, Natura 2000 conditionality, the Danish Green Tripartite — contracts the pre-reform capital stock by 60 percent at the calibrated arrival rate, and the joint-reform ranking extends across both regulatory margins.

The analysis treats a representative farm in partial equilibrium and abstracts from heterogeneous beliefs, financial frictions, and cross-sector spillovers. Agricultural capital is roughly two percent of Danish private capital, so general-equilibrium factor-price feedbacks are second-order, and partial equilibrium isolates the stranding mechanism. Arrival timing is exogenous and the subsidy is the only pre-regulation distortion; endogenising either weakens the quantitative magnitudes but preserves the reform ranking. The calibrated dynamic model is the baseline, with risk-neutral and frictionless cases reported as analytical benchmarks.

The irreversible-investment literature (Pindyck, 1988; Dixit and Pindyck, 1994; Abel and Eberly, 1996; Hassett and Metcalf, 1999; Bloom, 2009) establishes that policy uncertainty depresses investment; this paper adds endogenous subsidy capitalisation to the welfare comparison. Hong et al. (2023) model the destruction of productive capital under physical climate risk; the transition-risk channel formalised here is its anticipated-regulation counterpart. Learning over the timing of reform sits in the political-uncertainty tradition of Pástor and Veronesi (2012, 2013). The continuous-time framework follows Achdou et al. (2022).

The stranded-assets concept originated in fossil-fuel and energy contexts (McGlade and Ekins, 2015; van der Ploeg and Rezai, 2020; Welsby et al., 2021) and has developed mainly as a macro-finance object, with policy-risk pricing extensions (Rozenberg et al., 2020; Bolton and Kacperczyk, 2021; Barnett, 2023; Hambel and van der Ploeg, 2025) surveyed in Phan (2026). Agricultural stranding has received much less attention; Kortleve et al. (2025) document EU27 agricultural exposure empirically—the first systematic measurement at scale—but treat the loss as a static accounting object. Giglio et al. (2025b,a) show biodiversity risk is already priced in equity and CDS markets; the production-side counterpart is the stranded-capital cost of the subsidies that financed the physical exposure. In agricultural economics, Kirwan (2009), Hendricks et al. (2014), and Annan and Schlenker (2015) document subsidy capitalisation and insurance moral hazard in the United States; Ciaian and Kancs (2012) document analogous capitalisation of CAP area payments in Europe. Heterogeneous beliefs (Baldauf et al., 2020; Bakkensen et al., 2025) and financial frictions (Phan and Schwartzman, 2024; Kim et al., 2025) extend the partial-equilibrium setting.

The paper extends the agricultural-stranding literature on three margins. Pre-reform subsidies are the engine of the stranding magnitude: they pull the capital stock to a level that becomes excess once a tax arrives. Convex adjustment and partial irreversibility turn that excess into a welfare cost

that grows faster than linearly, with an order-of-magnitude amplification at the calibrated subsidy. The dynamic welfare framework then delivers a reform ranking: joint reform across direct-payment, insurance, and biodiversity-enforcement subsidies dominates sequential reform.

Section 2 sets up the model; Section 3 derives the analytical results; Section 4 delivers the baseline calibration, numerical solution, stranding-loss profile, and welfare counterfactuals; Section 5 reports the insurance and biodiversity extensions and the parameter-sensitivity and robustness checks; Section 6 concludes. Appendices contain proofs, the insurance and biodiversity derivations, robustness checks, and the cross-country portability exercise.

2 Model

A representative farmer accumulates capital under the threat of a policy regime switch. She receives a CAP-style per-unit subsidy ex ante; at a random future date the subsidy is withdrawn and a carbon tax arrives. Capital is partially irreversible, so the stock held at arrival generates a welfare loss that propagates through the post-regulation value function. The curvature of that value function determines the magnitude of the loss. The empirical setting is Danish dairy in 2024: the carbon tax was legislated in 2024 and takes effect in 2030, so the calibration anchors the pre-regulation regime to current data and the model projects the post-2030 transition. All proofs are in Appendix B.

2.1 Stranding Loss

Let $W(K)$ denote the post-regulation value function: discounted lifetime utility under capital stock K once the tax has been imposed. The model features three steady-state stocks: K_∞, the long-run stock under the post-regulation regime; K^*, the long-run stock under the pre-regulation regime with the CAP subsidy s; and K^0, its no-subsidy counterpart. When the post-regulation user cost exceeds the pre-regulation one, $K_\infty < K^0 < K^*$. The farmer holds K_T at the moment of regulation arrival, and the overhang $K_T - K_\infty > 0$ is the source of welfare loss.

The cost of the overhang is not the naive gap $W(K_\infty) - W(K_T)$, which blends misallocation with the level effect from the larger capital base at K_T. The Harberger-triangle correction (Hines, 1999) values each unit of overhang at its post-regulation marginal price $W'(K_\infty)$ and subtracts that linear shadow from actual welfare. The result is the *stranding loss*,

$$\mathcal{L}(K_T) \equiv \underbrace{W(K_\infty) + W'(K_\infty)(K_T - K_\infty)}_{\text{tangent at } K_\infty} - W(K_T). \tag{1}$$

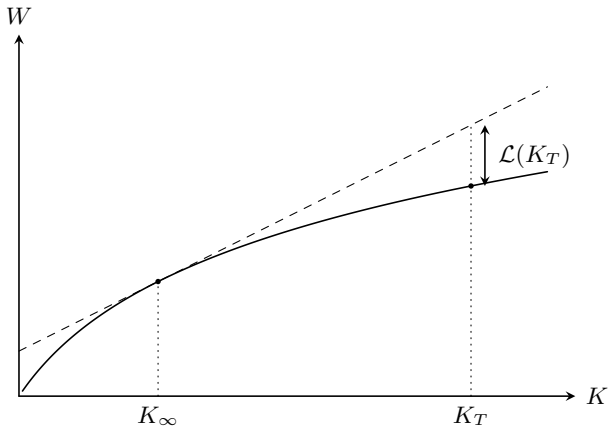

Figure 1: Stranding loss as a Harberger triangle. Dashed line: tangent to W at K_∞. The vertical gap $\mathcal{L}(K_T)$ between tangent and curve measures the convex residual; strict concavity of W ($W'' < 0$) is equivalent to strict convexity of $\mathcal{L}$.

The residual is non-negative because concavity of W puts the curve below its tangent except at the touch-point. Differentiating (1) twice with respect to K_T gives the curvature identity

$$\mathcal{L}''(K_T) \;=\; -W''(K_T) \;=\; |W''(K_T)|, \tag{2}$$

so strict concavity of W is equivalent to strict convexity of $\mathcal{L}$. Integrating twice under the boundary conditions $\mathcal{L}(K_\infty) = \mathcal{L}'(K_\infty) = 0$ delivers a closed form for the loss:

$$\mathcal{L}(K_T) \;=\; \int_{K_\infty}^{K_T} (K_T - z)\,|W''(z)|\,\mathrm{d}z. \tag{3}$$

The stranding loss is the $|W''|$-weighted first moment of distance to K_T on $[K_\infty, K_T]$. Equation (3) holds on intervals where $W \in C^2$ and strictly concave, covering the dynamic problem under convex adjustment and the two-risk joint CAP-and-biodiversity reform problem (Appendix C). In the frictionless limit, where adjustment costs vanish but the resale wedge remains, W is linear above the inaction boundary, the integral formula breaks on the linear region, and the loss is given in closed form by Proposition 2.9(i).

Proposition 2.1. *Let $W \in C^2$ with $W''(z) < 0$ on an open interval $\mathcal{I}$ containing the closed segment $[\min\{K_\infty, K_T\}, \max\{K_\infty, K_T\}]$. Then $\mathcal{L}$ is C^2 on $\mathcal{I}$, strictly convex in K_T, and strictly increasing for $K_T > K_\infty$, with*

$$\mathcal{L}(K_T) \;\geq\; \tfrac{1}{2}\,\underline{w}\,(K_T - K_\infty)^2, \qquad \underline{w} \equiv \inf_{z \in [\min\{K_\infty, K_T\},\, \max\{K_\infty, K_T\}]} |W''(z)| > 0. \tag{4}$$

If in addition $W \in C^3$ on $\mathcal{I}$, then near K_∞,

$$\mathcal{L}(K_T) \;=\; \tfrac{1}{2}|W''(K_\infty)|\,(K_T - K_\infty)^2 + O\big((K_T - K_\infty)^3\big). \tag{5}$$

When $|W''|$ is approximately constant on the overhang interval, the amplification multiplier $\mathcal{M}(s) \equiv \mathcal{L}(K^*(s))/\mathcal{L}(K^0)$ scales with the *square* of the overhang ratio rather than the ratio itself: subsidy-induced overhangs translate into superlinearly larger welfare losses. The adjustment technology determines the magnitude of $|W''|$, with the three regimes — frictionless liquidation, convex adjustment, and full irreversibility — developed in Section 2.3. Composing $\mathcal{L}$ with a joint-reform map yields the complementarity of CAP and biodiversity reform.

2.2 Static Liquidation Benchmark

A representative farmer chooses the capital stock K to maximise the per-period flow under the threat of a policy regime switch. Production is Cobb–Douglas, $\pi(K) = AK^\alpha$ with $\alpha \in (0,1)$. Capital is purchased at the replacement price p and resold at λp with $\lambda \in (0,1)$; the wedge $(1-\lambda)$ stands in for thin secondary markets, specialised equipment, and sunk structures (Abel and Eberly, 1996). Capital depreciates at rate δ, and the rate of time preference is ρ. The regime switch arrives as a Poisson event with hazard μ: at arrival the subsidy is withdrawn and a per-unit carbon tax τ is imposed. Capital is rebalanced instantaneously through the resale wedge, so the decision reduces to a static first-order condition in K; the dynamic model with convex adjustment costs is built in §2.3.

The farmer's per-period flow is

$$F(K,s) \;\equiv\; \pi(K) \;+\; sK \;-\; \underbrace{(\rho+\delta)\,p\,K}_{\text{Jorgensonian rental cost}} \;-\; \underbrace{\mu(1-\lambda)\,p\,K}_{\substack{\text{Poisson stranding}\\ \text{premium}}}. \tag{6}$$

The Jorgensonian term is the standard rental cost of capital — interest ρp plus depreciation δp per unit. The *Poisson stranding premium* $\mu(1-\lambda)p$ is the expected per-period capital loss at policy arrival: with hazard μ the regime ends, and the farmer can recover only λp of each unit she then liquidates. The premium is charged in advance through the no-arbitrage condition.

Maximising F over K in each regime delivers the three steady-state stocks of Section 2.1 as static first-order conditions:[1]

$$\pi'(K^0) = D, \tag{7}$$

$$\pi'(K^*) + s = D, \tag{8}$$

$$\pi'(K_\infty) = \tau + (\rho+\delta)p, \tag{9}$$

[1] Both τ and s are modelled as per-unit-of-livestock-capital instruments. For the carbon charge this is literal when emissions scale with herd size (≈ 6 tCO_2e/cow/yr). For CAP support it is a reduced-form pass-through assumption: only the component of total farm support capitalised into the livestock-capital composite enters s. Letting S denote total CAP support per livestock unit and $\chi_s \in [0,1]$ the pass-through into livestock capital,

$$s \;=\; \chi_s\, S.$$

Because most CAP income support (BISS, eco-schemes) is area-based and decoupled and capitalises predominantly into land rents (Kirwan, 2009; Ciaian and Kancs, 2012), the benchmark $\chi_s = 1$ in Section 4.1 should be read as an *upper-bound* livestock-capitalisation case. Section 5.3 reports the sensitivity over $\chi_s \in \{0.25, 0.50, 0.75, 1\}$.

Table 1: Static benchmark: capital and stranding losses

Target	K (LU)	$K - K_\infty$ (LU)	$\mathcal{L}^{\text{stat}}$ (EUR '000)
K_∞ (post-regulation)	21.3	—	—
$\bar{K}^{\text{RN}}$ (risk-neutral inaction boundary)	29.0	7.7	12.3
K^0 (no subsidy)	49.4	28.1	44.9
K^* (CAP subsidy)	207.1	185.8	297.3
Amplification $\mathcal{M}^{\text{stat}} = (K^* - K_\infty)/(K^0 - K_\infty)$			6.6×

Notes: Targets ordered by capital level. Stranding loss $\mathcal{L}^{\text{stat}}$ from equation (11). Parameters from Table 4.

with $D \equiv (\rho + \delta)p + \mu(1 - \lambda)p$ the total user cost. The pre-regulation FOCs differ only in the subsidy: s lowers the effective marginal cost from D to $D - s$, raising the target from K^0 to K^*. The post-regulation FOC drops the Poisson stranding premium (the event has occurred) and adds the tax τ, lowering the target to K_∞.

The resale wedge creates a region of inaction in which the farmer prefers to hold her stock rather than buy or sell. The risk-neutral upper boundary, denoted $\bar{K}^{\text{RN}}$ to distinguish it from the calibrated CRRA boundary $\bar{K}^{\text{CRRA}}$ of §2.4, is the largest capital stock at which holding still dominates selling at the resale price λp, and solves

$$\pi'(\bar{K}^{\text{RN}}) \;=\; \tau + (\rho + \delta)\,\lambda p. \tag{10}$$

Above $\bar{K}^{\text{RN}}$ marginal product has fallen far enough that liquidating dominates depreciating in place; on $[K_\infty, \bar{K}^{\text{RN}}]$ the farmer holds her stock fixed, and the band width measures the irreversibility wedge.

Under instantaneous liquidation, the stranding loss is the per-unit resale wedge applied to the overhang at the post-regulation target:

$$\mathcal{L}^{\text{stat}}(K_T) \;=\; (1 - \lambda)\,p \cdot (K_T - K_\infty)^+. \tag{11}$$

The loss is linear in K_T at the per-unit rate $(1 - \lambda)p$, equal to 1.6 EUR '000/LU at the calibrated $\lambda = 0.60$ and $p = 4$.

Proposition 2.2. *Under instantaneous portfolio rebalancing and $\mu(1 - \lambda)p < \tau$ (which ensures $K^0 > K_\infty$), the static amplification multiplier is*

$$\mathcal{M}^{\text{stat}} \;\equiv\; \frac{\mathcal{L}^{\text{stat}}(K^*)}{\mathcal{L}^{\text{stat}}(K^0)} \;=\; \frac{K^* - K_\infty}{K^0 - K_\infty}. \tag{12}$$

Inverting the Cobb–Douglas FOCs in (7)–(9) delivers closed-form steady-state stocks. At calibrated parameters (Table 1), the CAP subsidy closes 58% of the user-cost wedge, expands the steady-state herd from $K^0 = 49.4$ to $K^* = 207.1$ — a factor of four — and lifts the static ampli-

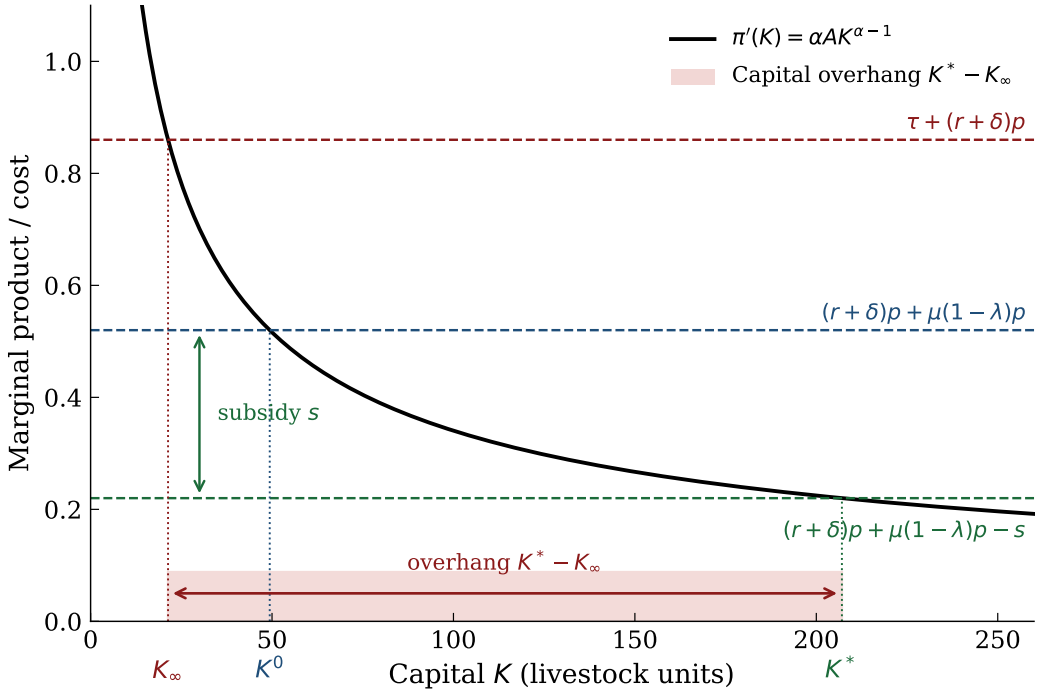

Figure 2: Three cost thresholds on the marginal-product curve. Shaded area: capital overhang ΔK.

fication multiplier to $\mathcal{M}^{\text{stat}} = 6.6$.[2] The linearity of $\mathcal{L}^{\text{stat}}$ is an artefact of valuing every overhang unit at the same wedge; Section 4.3 compares this static benchmark against the nested frictionless and full dynamic losses.

2.3 Dynamic Setting

Reform finds the farmer with capital that cannot be unwound costlessly: convex adjustment costs slow investment and disinvestment, preferences have curvature, and capital is exposed to Brownian shocks.

Preferences. The farmer has CRRA preferences with relative risk aversion $\gamma \geq 0$ and discount rate $\rho > 0$:

$$\mathbb{E}_0\left[\int_0^\infty e^{-\rho t}\, u(c_t)\, \mathrm{d}t\right], \qquad u(c) = \begin{cases} c^{1-\gamma}/(1-\gamma) & \gamma \notin \{0,1\}, \\ \ln c & \gamma = 1, \\ c & \gamma = 0. \end{cases}$$

Technology. Operating profit $\pi(K)$, net of variable inputs, satisfies $\pi' > 0$, $\pi'' < 0$, and Inada

[2]The 58% wedge reduction is $s/D = 0.30/0.52$. Under Cobb–Douglas, K^* has elasticity $1/(1-\alpha) = 5/3$ with respect to the user cost at $\alpha = 0.40$. The hypothesis $\mu(1-\lambda)p < \tau$ underlying Proposition 2.2 holds at calibrated values, $0.16 < 0.50$.

conditions. Capital evolves as

$$\mathrm{d}K_t = (I_t - \delta K_t)\,\mathrm{d}t + \sigma K_t\,\mathrm{d}Z_t, \tag{13}$$

with Z_t a standard Brownian motion, $\delta > 0$, $\sigma \geq 0$.[3] Total investment expenditure is

$$C(I, K) \;=\; \tilde{p}(I)\, I + \tfrac{\phi}{2}\,\frac{I^2}{K}, \qquad \phi \geq 0, \tag{14}$$

where the unit price

$$\tilde{p}(I) \;=\; \begin{cases} p & I \geq 0, \\ \lambda p & I < 0, \end{cases} \qquad \lambda \in (0, 1), \tag{15}$$

records the purchase–resale wedge: capital is bought at p and sold at $\lambda p < p$. Capital is measured in livestock units.[4]

Policy risk. A regime switch arrives at random time $T \sim \mathrm{Exp}(\mu)$, $\mu > 0$. At arrival, a permanent per-unit carbon tax $\tau > 0$ is imposed and the pre-regulation subsidy s is reduced to a residual level $s_r \in [0, s]$. The net policy shock is

$$\Delta \;\equiv\; \tau + (s - s_r). \tag{16}$$

The baseline sets $s_r = 0$; Table 13 reports $s_r \in \{0, 0.10, 0.15, 0.30\}$.[5]

Information. The farmer knows μ and τ.[6]

The farmer's budget constraint is

$$c_t = \begin{cases} c_t^0 & t < T, \\ c_t^1 & t \geq T, \end{cases} \tag{17}$$

with pre- and post-regulation consumption

$$c_t^0 = \pi(K_t) + sK_t - C(I_t, K_t), \qquad c_t^1 = \pi(K_t) - \tau K_t + s_r K_t - C(I_t, K_t).$$

2.4 Post-Regulation

After the regime switch, the farmer inherits K_T and solves the post-regulation control problem. With residual subsidy $s_r \in [0, s]$ persisting after arrival, the value function $W(K)$ satisfies the HJB

[3] Z aggregates physical shocks to the capital stock—animal-health, biological, and equipment risk—distinct from market-price risk (which enters through π) and from tax-severity risk (Appendix A.3). Brownian increments capture routine year-on-year variation; catastrophic events would require a jump-diffusion extension outside the baseline.

[4] K is a Hicks composite of livestock and farm structures; bundle weights and the implied (p, λ, δ) are in Section 4.1.

[5] Carbon taxation and subsidy reform are set by different authorities on different timelines, so partial bundling is empirically relevant: $s_r = 0$ corresponds to full bundling, $s_r = s$ to CAP persistence, intermediate values to partial reform. All analytical results hold with τ replaced by $\tau - s_r$ in the post-regulation problem.

[6] Appendix A relaxes both, with the baseline as the zero-variance limit.

equation

$$\rho W(K) = \max_I \{u(\pi(K) - (\tau - s_r)K - C(I,K)) + W'(K)(I - \delta K) + \tfrac{1}{2}\sigma^2 K^2 W''(K)\}. \quad (18)$$

The baseline sets $s_r = 0$, so the effective post-regulation charge is τ; Table 13 reports $s_r \in \{0, 0.10, 0.15, 0.30\}$.

The first-order condition in I equates the marginal continuation value of capital with the marginal cost of investment,

$$W'(K) = u'(c)\, C_I(I^*, K). \quad (19)$$

Dividing by $u'(c)$ converts utils to consumption goods and defines Tobin's marginal q,

$$q(K) \equiv \frac{W'(K)}{u'(c(K))} = C_I(I^*(K), K), \quad (20)$$

the shadow price of installed capital. From the cost specification (14)–(15), the marginal cost is $C_I(I,K) = \tilde{p}(I) + \phi I/K$, with right derivative p and left derivative λp at $I = 0$ and subdifferential $[\lambda p, p]$. Inverting $q = C_I$ across the kink delivers the three-region policy

$$I^*(K) = \begin{cases} (q-p)K/\phi & \text{if } q > p \quad \text{(positive investment)}, \\ 0 & \text{if } q \in [\lambda p, p] \quad \text{(inaction)}, \\ (q - \lambda p)K/\phi & \text{if } q < \lambda p \quad \text{(disinvestment)}. \end{cases} \quad (21)$$

The inaction band $q \in [\lambda p, p]$ is the kink subdifferential (Abel and Eberly, 1996); the wedge $(1-\lambda)p$ opens it and is the per-unit irreversibility cost paid on every liquidated unit.

The deterministic post-regulation problem has a long-run target at which replacement investment offsets depreciation and the drift of K vanishes.

Definition 2.3. A *zero-drift target* is a capital level $K_\infty > 0$ at which $I^*(K_\infty) = \delta K_\infty$, equivalently $q(K_\infty) = p + \phi\delta$.

In the deterministic case, the target exists, is unique, and is pinned by marginal product equating the post-tax user cost augmented by a convex-adjustment premium. Under $\sigma > 0$, the same level shifts by an $O(\sigma^2)$ stochastic correction (Remark B.2).

Proposition 2.4. *Let $\tau_{\text{eff}} \equiv \tau - s_r$. With $\sigma = 0$, the post-regulation problem has a unique zero-drift target $K_\infty(\tau_{\text{eff}}) > 0$ characterized by*

$$\pi'(K_\infty) = \tau_{\text{eff}} + (\rho + \delta)(p + \phi\delta) - \tfrac{1}{2}\phi\delta^2. \quad (22)$$

The baseline sets $s_r = 0$, so $\tau_{\text{eff}} = \tau$; Table 13 reports $s_r \in \{0, 0.10, 0.15, 0.30\}$.

Expanding (22), $\pi'(K_\infty) = \tau_{\text{eff}} + (\rho + \delta)p + \phi\delta(\rho + \delta/2)$. The convex-adjustment premium $\phi\delta(\rho + \delta/2)$ vanishes at $\phi = 0$, recovering the static FOC (9).[7]

[7] At calibration the premium is small not because $\phi\delta$ is small but because of the factor $\rho + \delta/2$, and shifts K_∞

Inaction band. The optimal policy is characterized by the position of Tobin's marginal q relative to the purchase and resale prices. If $q > p$, the farmer invests; if $q < \lambda p$, she disinvests; and if $q \in [\lambda p, p]$, the kinked adjustment cost supports inaction. The boundaries of the inaction band are the capital levels at which q reaches p and λp. At the zero-drift target $q(K_\infty) = p + \phi\delta > p > \lambda p$, so K_∞ lies on the investment branch.

Lemma 2.5. *Suppose $\tau_{\text{eff}} > 0$, $\phi > 0$, $\lambda \in (0,1)$. Assume utility is defined on strictly positive consumption and the post-regulation tail is feasible: there exists $a > 0$ such that*

$$\lambda p\, a - \frac{\phi}{2} a^2 > \tau_{\text{eff}}. \tag{23}$$

Let q be continuous on $[K_\infty, \infty)$ and satisfy $q(K_\infty) = p + \phi\delta$. Then there exist K_p and $\bar{K}$ such that[8]

$$K_\infty < K_p < \bar{K}, \qquad q(K_p) = p, \qquad q(\bar{K}) = \lambda p. \tag{24}$$

Condition (23) is a feasibility restriction on the post-regulation upper tail; its calibrated value is reported in Remark B.1(ii).

Uniqueness of $(K_p, \bar{K})$ requires single-crossing of q at p and λp. At points of differentiability, $q(K) = W'(K)/u'(c^1(K))$, and under CRRA, $-u''(c^1)/u'(c^1) = \gamma/c^1$, so

$$q'(K) = \frac{W''(K)}{u'(c^1(K))} + \gamma\, q(K)\, \frac{(c^1)'(K)}{c^1(K)}. \tag{25}$$

The second term in (25) can be positive on the investment branch, so concavity of W alone does not yield $q' < 0$ under CRRA. Lemma 2.6 delivers local uniqueness from stability of the deterministic flow at K_∞ and global uniqueness in the risk-neutral benchmark from concavity of W; under calibrated CRRA preferences, global single-crossing is verified numerically (Remark B.1(i)).

Lemma 2.6. *Let the hypotheses of Lemma 2.5 hold.*

(i) *Suppose $\sigma = 0$ and q is C^1 on a neighbourhood of K_∞. If the deterministic post-regulation drift $\dot{K} = K(r(K) - \delta)$, with $r(K) \equiv I^*(K)/K$, is locally asymptotically stable at K_∞, then q is strictly decreasing on some neighbourhood U of K_∞; equivalently, the level set $\{K \in U : q(K) = y\}$ is a singleton for every $y \in q(U)$.*

(ii) *If q single-crosses the levels p and λp on $[K_\infty, \infty)$, the thresholds in (24) are unique. In the deterministic risk-neutral benchmark, $q = W'$ and Assumption 2 gives $q'(K) = W''(K) < 0$ on the overhang interval, so the crossings are globally unique.*

down by about three percent: $\phi\delta(\rho + \delta/2) = 0.016$ against $(\rho + \delta)p = 0.36$, with $\phi\delta = 0.25$ and $\rho + \delta/2 = 0.065$. The diffusion correction at $\sigma = 0.04$ is of order 10^{-3}; the numerical convergence rate is $\eta_\sigma \approx 0.300$ against the deterministic $\eta = 0.302$, and $\mathbb{E}[|K_t - K_\infty|]$ decays at $\approx 0.20\,\text{yr}^{-1}$ (half-life 3.5 years), confirmed by Monte Carlo with 10^4 paths.

[8] Stated at $\sigma = 0$. Under $\sigma > 0$, the implicit function theorem applied to the stochastic FOC at the deterministic root gives $K_p^\sigma = K_p + O(\sigma^2)$ and $\bar{K}^\sigma = \bar{K} + O(\sigma^2)$ as $\sigma \to 0$, since the stochastic correction $\frac{1}{2}\sigma^2 K^2 W''(K)$ in the HJB is itself $O(\sigma^2)$.

The induced policy partitions $[0, \infty)$ into four regions (Table 2).

Table 2: Optimal post-regulation policy regions.

Region	**Capital** K	**Shadow value** q	**Investment** I^*	**Drift** $\dot{K}$
Accumulation	$K < K_\infty$	$q > p + \phi\delta$	$I^* > \delta K$	> 0
Slow investment	$K \in (K_\infty, K_p)$	$q \in (p, p + \phi\delta)$	$0 < I^* < \delta K$	< 0
Inaction	$K \in [K_p, \bar{K}]$	$q \in [\lambda p, p]$	$I^* = 0$	$-\delta K$
Disinvestment	$K > \bar{K}$	$q < \lambda p$	$I^* < 0$	$< -\delta K$

2.5 Pre-Regulation

Before the tax arrives, the farmer receives the subsidized flow payoff $\pi(K_t) + sK_t - C(I_t, K_t)$ and faces the prospect of regime termination at T with continuation value W. The pre-regulation value function is

$$V(K) = \max_{\{I_t\}} \mathbb{E}\left[\int_0^T e^{-\rho t} u(c_t^0)\,\mathrm{d}t + e^{-\rho T} W(K_T)\right], \tag{26}$$

subject to (13).

Lemma 2.7. *Let V be C^2 in K. Then*

$$(\rho+\mu)V(K) = \max_I \Big\{ u\big(\pi(K)+sK-C(I,K)\big) + V'(K)(I-\delta K) + \tfrac{1}{2}\sigma^2 K^2 V''(K) + \mu\, W(K) \Big\}, \tag{27}$$

The effective discount rate $\rho + \mu$ carries the regime-termination hazard, and $\mu W(K)$ is the expected continuation value at arrival.

Proposition 2.8. *Suppose $\gamma = \phi = \sigma = 0$ and $K^* > \bar{K}^{\mathrm{RN}}$.*[9] *Then $W'(K^*) = \lambda p$ and the pre-regulation target satisfies*

$$\pi'(K^*) + s \;=\; (\rho + \delta)p + \mu(1 - \lambda)p \;\equiv\; D. \tag{28}$$

Under CRRA with $\gamma > 0$, the marginal-utility weight on the post-liquidation resale payoff raises the pre-regulation target above the risk-neutral level (Proposition 2.10).

2.6 Limiting Cases

Three limits frame the parameter space: $\phi \downarrow 0$ delivers the frictionless free-boundary problem of Proposition 2.9(i) anchored at $\bar{K} > K_\infty$; $\phi \to \infty$ collapses investment to zero; $\lambda \to 1$ removes the irreversibility wedge.

For shocks of comparable fractional magnitude, the leading-order quadratic (5) implies that timing variance dominates magnitude variance by the ratio $(K^*/K_\infty)^2 \approx 95$ at calibration: strand-

[9] Sufficient condition: $s > D - \pi'(\bar{K}^{\mathrm{RN}})$. At the Danish calibration ($A = 13.49$, $\alpha = 0.40$, $\bar{K}^{\mathrm{RN}} = 29.0$), $D - \pi'(\bar{K}^{\mathrm{RN}}) \approx -0.196$, so $s = 0.30$ satisfies it with a wide margin.

ing is a first-order welfare problem only when $K^* \gg K_\infty$ — the regime in which K_∞ is insensitive to τ.

Under (5) with $|W''|$ approximately constant, the amplification multiplier $\mathcal{M}(s)$ of §2.1 admits the leading-order approximation

$$\mathcal{M}(s) \;\approx\; \left(\frac{K^*(s) - K_\infty}{K^0 - K_\infty}\right)^2. \tag{29}$$

Under Cobb–Douglas, $|W''(z)| \propto z^{\alpha-2}$ decays for $z \gg K_\infty$,[10] so (29) overstates the exact multiplier when the overhang is large; $\mathcal{M}$ is computed numerically throughout, with the quadratic formula serving as a local benchmark.

Proposition 2.9. *Let $\sigma = 0$, $\gamma = 0$.*

(i) *As $\phi \downarrow 0$, $W_\phi \to W_0$ uniformly on compact subsets of $(0,\infty)$, and for $K_T > \bar{K}$*

$$\mathcal{L}|_{\phi=0}(K_T) = (1-\lambda)p\,(K_T - \bar{K}) + \Omega(\bar{K}, K_\infty),$$

with $\Omega(\bar{K}, K_\infty) \equiv W_0(K_\infty) - W_0(\bar{K}) + p(\bar{K} - K_\infty) \geq 0$, equality iff $\lambda = 1$.

(ii) *As $\lambda \to 1$, $\bar{K} \to K_\infty$ and $\mathcal{L}^{\text{stat}} \to 0$.*

(iii) *As $\phi \to \infty$, $I^*(K) \to 0$ pointwise on compact sets, and W_ϕ converges on every compact subset of $(0,\infty)$ bounded away from zero to the no-investment value W_∞.*

Part (i) decomposes the frictionless loss into a sale component $(1-\lambda)p(K_T - \bar{K})$ — the resale discount on capital liquidated at the inaction boundary — and a depreciation-band component $\Omega(\bar{K}, K_\infty)$ — the present-value cost of letting K drift from $\bar{K}$ to K_∞ under zero investment. The latter vanishes only under perfect reversibility, where $\bar{K} = K_\infty$ and the static formula (11) is recovered. At the calibrated $\bar{K}/K_\infty = 1.36$ both components contribute. Part (iii) shows that $|W''|$ scales as $1/\phi$ in the q-theory limit while the overhang $K^* - K_\infty$ grows with ϕ; the product in (3) is bounded but need not be monotone. The envelope over ϕ is evaluated numerically in Table 11.

2.7 Consumption-Gap Amplification

Risk aversion enters the pre-regulation FOC through the marginal-utility weight on the post-regulation resale payout, raising K^* above the risk-neutral level through a channel distinct from standard precautionary saving.

The comparative statics below are local around the risk-neutral liquidation boundary $\bar{K}^{\text{RN}}$.

Proposition 2.10. *Assume Cobb–Douglas production, $\sigma = 0$, $\phi = 0$, $K^*(0) > \bar{K}^{\text{RN}}$, and the feasibility condition $c^0(K^*) > \tilde{c}^1 > 0$ in (30). On an open neighbourhood of $\gamma = 0$,*

[10] From the post-regulation FOC, $W''(z)$ — at any capital level z in the overhang interval $[K_\infty, K_T]$ — inherits the curvature of $\pi(z) = Az^\alpha$ at leading order in ϕ^{-1}, so $|W''(z)| = O(z^{\alpha-2})$.

(i) $\left.\dfrac{\partial K^*}{\partial \gamma}\right|_{\gamma=0} > 0$;

(ii) $\left.\dfrac{\partial^2 K^*}{\partial s\,\partial \gamma}\right|_{\gamma=0} > 0$.

At $\phi = 0$ with $K^* > \bar{K}^{\mathrm{RN}}$, the farmer instantaneously liquidates $K^* - \bar{K}^{\mathrm{RN}}$ at the resale price λp and then operates at $\bar{K}^{\mathrm{RN}}$, so the marginal utility weight on the resale payout is evaluated at $\bar{K}^{\mathrm{RN}}$.[11] Define the shadow consumptions $c^0(K) \equiv \pi(K) - (\delta p - s)\,K$ and $\tilde{c}^1 \equiv c^1(\bar{K}^{\mathrm{RN}}) \equiv \pi(\bar{K}^{\mathrm{RN}}) - (\tau + \delta\lambda p)\,\bar{K}^{\mathrm{RN}}$, dual to $V'(K) = u'(c^0)\,p$ and $W'(\bar{K}^{\mathrm{RN}}) = u'(\tilde{c}^1)\,\lambda p$. Assume

$$c^0(K^*) > \tilde{c}^1 > 0, \tag{30}$$

satisfied at baseline ($c^0(K^*) \approx 134$, $\tilde{c}^1 \approx 34$). Then $R(\gamma) \equiv u'(\tilde{c}^1)/u'(c^0(K^*)) = \omega^\gamma$ with $\omega \equiv c^0(K^*)/\tilde{c}^1$, and the pre-regulation FOC becomes

$$\pi'(K^*) + s \;=\; (\rho + \delta)p + \mu(1 - \lambda R)\,p, \tag{31}$$

collapsing to (28) at $\gamma = 0$. The utility-weighted recovery rate $\lambda R > \lambda$ shrinks the effective stranding premium and raises K^* — *consumption-gap amplification*. The closed-form FOC is local: $\lambda R(\gamma)$ crosses unity well below $\gamma = 2$ at calibrated ω and λ, so the full nonlinear effect is obtained from the HJB. At fixed A, the numerical solution yields a steady-state increase of roughly 8% at $\gamma = 2$, rising to 15–25% across $\gamma \in [1, 4]$, with a stranding-loss increase of approximately 17% at baseline. The cross-partial $\partial^2 K^*/\partial s\,\partial\gamma > 0$ confirms that subsidies and risk aversion are complements. Two exercises follow: at fixed A, raising γ raises K^*; in Table 21, $A(\gamma)$ is recalibrated to hold $K^* = 207.1$ fixed, isolating curvature effects on welfare from level effects on K^*.

3 Analytical Results

Specializing to Cobb–Douglas production, $\pi(K) = AK^\alpha$, gives closed-form steady states, convergence rates, and a money-metric planner's problem.

3.1 Steady States

Closed-form steady states obtain by inverting the FOCs of Propositions 2.4 and 2.8 under Cobb–Douglas.

Lemma 3.1. *Under Cobb–Douglas production ($\pi(K) = AK^\alpha$), risk neutrality ($\gamma = 0$), and deterministic capital ($\sigma = 0$), the post-regulation zero-drift target is*

$$K_\infty(\tau_{\mathrm{eff}}) = \left(\frac{\alpha A}{\tau_{\mathrm{eff}} + (\rho + \delta)(p + \phi\delta) - \frac{1}{2}\phi\delta^2}\right)^{1/(1-\alpha)}, \qquad \tau_{\mathrm{eff}} \equiv \tau - s_r. \tag{32}$$

[11] Holding K^* fixed would require the stand-alone flow $\pi(K^*) - (\tau + \delta\lambda p)K^*$, which is negative at the Danish calibration.

Specializing further to $\phi = 0$, the inaction boundary and subsidized target are

$$\bar{K}(\tau) = \left(\frac{\alpha A}{\tau + (\rho + \delta)\lambda p} \right)^{1/(1-\alpha)}, \tag{33}$$

$$K^*(\mu, s) = \left(\frac{\alpha A}{D - s} \right)^{1/(1-\alpha)}, \tag{34}$$

with $D \equiv (\rho+\delta)p+\mu(1-\lambda)p$. For $\phi\delta \ll (\rho+\delta)p$, (32) reduces to $K_\infty \approx (\alpha A/(\tau+(\rho+\delta)p))^{1/(1-\alpha)}$, and (33)–(34) remain accurate to the same order. Existence of a finite K^* requires $D > s$.

The Cobb–Douglas elasticity $1/(1-\alpha) = 5/3$ at the calibrated $\alpha = 0.40$ amplifies user-cost changes into capital changes: a 10% rise in the net user cost $D - s$ contracts K^* by 17%. The same elasticity drives the cross-country exercise of Appendix D, where heterogeneous (A_j, μ_j, s_j) map to country-specific (K_j^*, K_∞^j) pairs through the same inversion. Existence requires $D > s$; at the calibrated $D = 0.52$ and $s = 0.30$, the wedge $D - s = 0.22$ is well inside the existence region.

3.2 Dynamics

The deterministic post-regulation dynamics admit a local saddle-path linearization and a global Lyapunov bound.

Proposition 3.2. *Suppose $\gamma = 0$, $\sigma = 0$, and $\phi > 0$. Let K_∞ denote the deterministic post-regulation steady state from Proposition 2.4, and let $q \equiv W'(K) = p + \phi\, I/K$ denote the current-value shadow price. The linearised post-regulation dynamics around (K_∞, q_∞), where $q_\infty = p + \phi\delta$ from Definition 2.3, have one stable eigenvalue $-\eta < 0$, where*

$$\eta = \frac{-\rho + \sqrt{\rho^2 + 4|\pi''(K_\infty)|K_\infty/\phi}}{2}. \tag{35}$$

Hence, along the local saddle path, $K_t - K_\infty = O(e^{-\eta t})$, and the local half-life is $t_{1/2} = \ln 2/\eta$.

At the calibrated parameters $(\rho, \delta, \phi, \alpha, A) = (0.04, 0.05, 5, 0.40, 13.49)$, $\eta \approx 0.30$ and the local half-life is $\ln 2/\eta \approx 2.3$ years. The local rate underwrites the linearised welfare formula in §4.4. The calibrated $K^*/K_\infty = 9.7$ places the inherited stock far from the linearisation base point, so the full-transition welfare integrals require the global bound below.

Proposition 3.3. *Let $\sigma = 0$ and $\dot{K} = G(K) \equiv I^*(K) - \delta K$. If there exists $\underline{\eta} > 0$ such that*

$$(K - K_\infty)\, G(K) \le -\underline{\eta}\, (K - K_\infty)^2 \qquad \text{for all } K \ge 0, \tag{36}$$

then for every $K_0 \ge 0$,

$$|K_t - K_\infty| \le |K_0 - K_\infty|\, e^{-\underline{\eta} t}. \tag{37}$$

By the mean-value theorem, (36) holds whenever $G'(K) \le -\underline{\eta}$ for all $K \ge 0$. The condition is verified numerically on the computed policy function with $\underline{\eta} > 0$, so the welfare integral $\int_0^\infty e^{-\rho t} u(c_t)\, \mathrm{d}t$ converges absolutely along every transition path used in §4.3.

3.3 Optimal Policy

The planner internalises three margins: current environmental damages, the fiscal cost of the subsidy, and the effect of the subsidy on the farmer's capital accumulation before policy arrival. Define money-metric utility $\tilde{u}(c) \equiv u(c)/u'(\bar{c})$, where $\bar{c}$ is the pre-tax steady-state consumption level; this normalisation puts all three components of the objective in euros per year. The planner maximises

$$\mathcal{W} = \mathbb{E}_0 \left[\int_0^\infty e^{-\rho t} \big[\underbrace{\tilde{u}(c_t)}_{\substack{\text{money-metric} \\ \text{utility}}} - \underbrace{d(K_t)}_{\substack{\text{environmental} \\ \text{damage}}} - \underbrace{\xi\, s_t\, K_t}_{\substack{\text{fiscal cost} \\ \text{of subsidy}}} \big] \, \mathrm{d}t \right], \tag{38}$$

where $d(K) = \delta_e K$ is environmental damage and $\xi > 0$ is the marginal cost of public funds (MCPF), set to 0.30. A full characterisation of the Markov-perfect rule $s^*(K)$ requires solving the planner's problem jointly with the farmer's response; candidate subsidy paths are evaluated numerically.

Higher inherited capital raises the marginal social cost of the subsidy through both current environmental damages ($d'(K) = \delta_e$) and the capital overhang exposed to future stranding ($\partial \mathcal{L}/\partial K > 0$). Subsidy phase-out is a numerical conclusion of the solved model; the welfare ranking and the critical subsidy threshold are reported in §4.4.

4 Quantitative Analysis

Danish dairy farming is the empirical anchor: a homogeneous livestock capital stock, a single observable commodity, decades of standardised microdata, and a legislated carbon tax that identifies the post-regulation regime.

4.1 Data and Calibration

The calibration draws on three sources. The EU Farm Accountancy Data Network microdata (FADN, 2004–2023) supply the calibration moments: structures (SE005–SE080), income (SE131–SE430), subsidies (SE605–SE630), and financial indicators (SE501–SE526), for the specialist dairy type (TF8) across 27 member states.[12] EU ETS and Danish legislation discipline the τ scenario. Quarterly Danish farm investment accounts (Statistics Denmark, Jord2; 6,358 farm-year-quarter observations) document the investment rate and its dispersion across farm-size quartiles.

[12] The Danish panel covers 20 years of country-level averages summarised in Table 3; average herd size nearly doubled over the sample, and net farm income swings with commodity prices.

Table 3: Descriptive statistics: Danish dairy farms (FADN, 2004–2023)

Variable	Mean	Std	Min	Max	N_{years}
Panel A: Farm structure					
Cattle (head/farm)	266.6	68.1	154.3	358.0	20
UAA (ha/farm)	157.9	39.7	99.1	222.5	20
Economic size (EUR '000)	371.3	151.5	170.1	618.4	20
Farms represented	5,362	1,549	2,440	7,610	20
Panel B: Income and subsidies (EUR/farm)					
Total output	349,286	91,714	196,527	506,871	20
Net farm income	87,327	48,352	14,628	186,019	20
Total subsidies	70,961	8,987	51,203	88,432	20
Selected (non-exclusive) subsidy indicators†*:*					
Decoupled payments	39,155	8,224	20,813	51,780	20
Livestock-related support	63,599	7,623	48,121	78,441	20
Panel C: Capital and investment (EUR/farm)					
Average farm capital	1,617,923	433,189	947,561	2,318,752	20
Net worth	1,094,064	301,748	623,911	1,609,322	20
Gross investment	153,002	52,630	66,318	258,413	20
Investment rate (I/K)	0.097	0.023	0.055	0.142	20
Debt ratio ($1 - \text{NW}/K$)	0.319	0.041	0.250	0.386	20

Notes: Weighted by SYS02. †Decoupled and livestock-related indicators overlap and do not partition total subsidies; they are reported as non-exclusive aggregates within total support.

Capital as a Hicks composite. Capital K is measured in livestock units (LU), the EU standard equal to one adult dairy cow (≈500 kg). On a Danish dairy farm the bundle—livestock, barn, slurry, parlour—moves in roughly fixed proportions with value shares 0.55, 0.20, 0.10, and 0.15 respectively (FADN 2019–2023), which permits a Hicks composite with bundle-weighted primitives. The purchase price p = EUR 4K/LU is the 2019–2023 heifer price; $\lambda = 0.60$ is the auction-to-replacement discount on cull cattle; $\delta = 0.05$ is the value-weighted depreciation rate; ϕ is calibrated internally against the composite investment rate. Sensitivity to $\lambda \in \{0.40, 0.80\}$ is in Table 11; re-weighting shares by ±20 percentage points shifts (p, λ, δ) by at most five percent.

External targets set ρ, α, δ, p, and λ from the agricultural-economics literature and from Danish auction records; internal calibration uses the FADN panel to pin down A and ϕ. Table 4 reports the baseline parameters and Table 5 the implied steady states.

Table 4: Baseline calibration (monetary values in EUR '000; 1 LU $\approx$ 500 kg)

	Symbol	Value	Class	Source
Preferences and technology				
Discount rate	ρ	0.04	L	Standard
Risk aversion	γ	2.0	L	Standard
TFP (normalised)	A	13.49	I	Matches $K^* = 207$ LU in baseline HJB
Capital share	α	0.40	L	Mundlak (2001)
Depreciation	δ	0.05	O/A	Blended livestock/building
Purchase price	p	4.0	O	Danish Cattle Federation
Resale fraction	λ	0.60	O	Auction data (DAFC/SEGES)
Adjustment cost	ϕ	5.0	I	Matches FADN I/K
Capital volatility	σ	0.04	O	FADN panel
Policy				
Total CAP support per LU	S	0.30	O	FADN 2019–2023
Pass-through to livestock capital	χ_s	1.00	A	Upper-bound benchmark
Livestock-capital subsidy	$s = \chi_s S$	0.30	I/A	Effective user-cost wedge
Carbon tax	τ	0.50	S	DK legislation (long-run)
Arrival rate	μ	0.10	A	Belief about reform timing
MCPF	ξ	0.30	L	Rozenberg et al. (2020)
Damage rate	δ_e	0.20	A	Methane damages per LU
Insurance subsidy (French Assurance Récolte)				
Premium subsidy rate	ζ	0.70	O	Enjolras and Sentis (2023)
Cost pass-through	ψ	0.85	A	Assumption
Capital-cost wedge	s_{ins}	0.027	I	$\psi\zeta\,\mathbb{E}[\lambda_a]D_a$

Class: O observed; L literature central estimate; I internally calibrated to a moment; A assumption; S policy scenario. Sensitivity to the assumption parameters μ and δ_e is in Tables 19 and 11.

Table 5: Implied steady states at baseline calibration

	Symbol	Value	Formula
Pre-regulation, calibrated HJB	K^*	207.1 LU	numerical, $(\gamma, \phi, \sigma) = (2, 5, 0.04)$
Pre-regulation, RN diagnostic	$K^{*,\mathrm{RN}}$	≈ 192 LU	$(\alpha A/(D-s))^{1/(1-\alpha)}$
No-subsidy, RN diagnostic	$K^{0,\mathrm{RN}}$	49.4 LU	$(\alpha A/D)^{1/(1-\alpha)}$
No-subsidy, calibrated HJB	$K^{0,\mathrm{HJB}}$	49.4 LU	numerical, $(\gamma, \phi, \sigma) = (2, 5, 0.04)$
Post-regulation, calibrated HJB	K^{ϕ}_{∞}	20.7 LU	$(\alpha A/[\tau + (\rho+\delta)(p+\phi\delta) - \frac{1}{2}\phi\delta^2])^{1/(1-\alpha)}$
Post-regulation, RN diagnostic	K^{0}_{∞}	21.3 LU	$(\alpha A/(\tau + (\rho+\delta)p))^{1/(1-\alpha)}$
Inaction boundary, RN analytical	$\bar{K}^{\mathrm{RN}}$	29.0 LU	$(\alpha A/(\tau + (\rho+\delta)\lambda p))^{1/(1-\alpha)}$
Inaction boundary, calibrated CRRA	$\bar{K}^{\mathrm{CRRA}}$	≈ 54 LU	numerical
User cost	D	0.52	$(\rho+\delta)p + \mu(1-\lambda)p$
Convergence rate	η	0.302	$t_{1/2} = 2.3$ yr

Notes: The productivity scale $A = 13.49$ is calibrated in the full CRRA HJB at $(\gamma, \phi, \sigma) = (2, 5, 0.04)$ to match $K^* = 207.1$ LU (the 2019 Danish dairy herd). The risk-neutral closed-form values are reported as analytical diagnostics at the same A; under CRRA the consumption-gap channel raises K^* above the RN diagnostic by roughly 8% (§2.7), and similar discrepancies appear at the post-regulation boundary $\bar{K}^{\mathrm{CRRA}} > \bar{K}^{\mathrm{RN}}$. At $s = 0$ the consumption-gap correction is below table-rounding precision: $K^{0,\mathrm{HJB}} = 49.4$ LU coincides with the RN value $K^{0,\mathrm{RN}} = 49.4$ LU to three significant figures, since the post-tax consumption floor and resale wedge are nearly identical at the no-subsidy steady state. The dynamic target K^{ϕ}_{∞} is roughly 3% below the frictionless K^{0}_{∞} owing to the convex-adjustment premium $\phi\delta(\rho + \delta/2)$. The amplification multiplier $\mathcal{M} = \mathcal{L}(K^*)/\mathcal{L}(K^{0,\mathrm{HJB}})$ uses the calibrated-HJB no-subsidy value throughout.

The discount rate $\rho = 0.04$ follows agricultural finance practice (USDA Economic Research Service, 2020). The depreciation rate $\delta = 0.05$ is a *net* rate on the composite stock: gross depreciation runs at 14–20%/yr on the herd (5–7 yr productive life) and 2.5–5%/yr on barn, parlour, and slurry capacity (20–40 yr life), but heifer replacement rolls culled cows back into the stock at cost p, and the net flow matches the FADN implied rate. The replacement cost $p = 4.0$ is the 2019–2023 average replacement-heifer price (Danish Cattle Federation); the resale fraction $\lambda = 0.60$ reflects the 30–50% auction discount (Danish Agriculture and Food Council, SEGES Innovation). The capital share $\alpha = 0.40$ lies within the 0.25–0.45 range used in agricultural production-function estimation (Griliches, 1963; Mundlak, 2001). The TFP level $A = 13.49$ is normalised so that K^* matches the average Danish milking herd of 207 LU in 2019; $\phi = 5.0$ is calibrated internally against the 5–8% gross investment rate observed in the pre-tax 2010–2019 sub-sample (Table 6), rather than the 9.7% full-sample mean in Table 3, which includes the 2020–2023 expansion. The capital volatility $\sigma = 0.04$ is the year-on-year coefficient of variation of herd size in the 2010–2019 FADN sub-sample.

The CAP support figure $S = 0.30$ (EUR 300/LU/yr) scales FADN total subsidies SE605 (EUR 71,000/farm) by the 2019–2023 average milking herd of ≈ 240 LU; using the 2019 anchor $K^* = 207$ LU directly gives $S \approx 0.343$, $A = 10.85$, and $\mathcal{M} \approx 20.8$. The baseline sets the pass-through $\chi_s = 1$, so the livestock-capital subsidy is $s = \chi_s S = 0.30$; this is an upper-bound calibra-

tion because most CAP income support is area-based and decoupled and capitalises into land rents rather than into the livestock-capital composite (Section 5.3 reports the $\chi_s \in \{0.25, 0.50, 0.75, 1\}$ pass-through grid). The carbon tax $\tau = 0.50$ (EUR 500/LU/yr) targets a long-run rate at which the current 60% deduction has been phased out; $\tau = 0.24$ brackets the results in Section 5.3. The arrival rate $\mu = 0.10$ matches the pre-2020 Danish policy environment in which no agricultural carbon tax was under active consideration; Appendix A.1 maps the 2020–2024 Danish legislative sequence into the Gamma–Poisson posterior. Insurance-subsidy parameters $(\zeta, \psi, s_{\text{ins}})$ are defined in Section 5.1. The damage rate $\delta_e = 0.20$ coincides with the zero-subsidy threshold of §4.4.

Against the backdrop of EU ETS prices that rose from EUR 20–25/tCO_2 in 2005 to EUR 65–85 in 2025, Denmark's agricultural carbon tax is legislated at headline rates of DKK 300/tCO_2e (EUR 40) from 2030 and DKK 750 (EUR 100) from 2035, subject to a 60% basic deduction on a statutory emissions base of roughly 6 tCO_2e per animal; the effective per-LU charge is EUR 16/tCO_2e in 2030 and EUR 40/tCO_2e in 2035. The 6 tCO_2e statutory base is the regulatory tax parameter and is narrower than the 10.4 tCO_2e/LU/yr full life-cycle factor used in the Section 3.3 social-cost calculation, which incorporates enteric and manure methane under 100-year GWP. Appendix D applies the calibration to four other EU jurisdictions.

Table 6: Model fit

Moment	**Data**	**Model**	**Source**
Targeted			
Avg. milking cows/farm	≈207	207.1	Danish Ag. Council (2019)
Net depreciation rate	≈5%	5.0%	Equipment/livestock life
Untargeted			
Net farm income (EUR '000/yr)	50–190	133.3	FADN SE425 (2004–2023)
Gross investment rate I/K	5–8%	5.0%	FADN SE516/SE510 (2010–2019)

Notes: SE080 counts total cattle including heifers. The 207-LU milking-cow calibration target is taken from the Danish Agriculture Council 2019 benchmark and is not obtained by applying a fixed conversion to the 2004–2023 FADN average reported in Table 3. The gross investment rate sits at the low end of the data range because the model collapses multiple capital goods into one stock.

4.2 Numerical Solution

The post-regulation HJB (18) is solved first and supplies the continuation value for the pre-regulation HJB (27). Both equations are solved by implicit finite differences with an upwind discretisation of the drift and central differences for the diffusion term, following Achdou et al. (2022). The baseline grid has $N = 500$ points on $[0.5, 260]$ LU; convergence is declared at tolerance 10^{-8} after 10–20 iterations. Doubling the grid to $N = 1000$ changes the baseline stranding loss $\mathcal{L}(K^*)$ by less than 0.3%, and the steady-state identity $W(K_\infty) = u(c_\infty)/\rho$ holds to within 0.5% under the calibrated $\sigma = 0.04$. The risk-neutral closed-form steady states of Lemma 3.1 match the

finite-difference solution to four decimal places, and the calibrated CRRA HJB shifts the inaction boundary from $\bar{K}^{\mathrm{RN}} = 29$ to $\bar{K}^{\mathrm{CRRA}} \approx 54$. Appendix F gives the discretised system, the upwind matrix structure, and the boundary-condition treatment.

4.3 Baseline Stranding Loss

The numerical solution delivers the value and policy functions, the stranding-loss profile, and the amplification multiplier $\mathcal{M} = 13.2$.

Value and policy functions. Both value functions W and V (Figure 3) are increasing and concave; under CRRA with $\gamma = 2$, $u(c) = -1/c$, so all values are negative. Both are increasing throughout the grid — even far above the post-regulation optimum — because excess capital can be sold at λp, generating consumption during the transition. The gap $V(K) - W(K)$ widens with K: larger farms capture more of the proportional subsidy and hold greater option value from optimal pre-arrival adjustment.

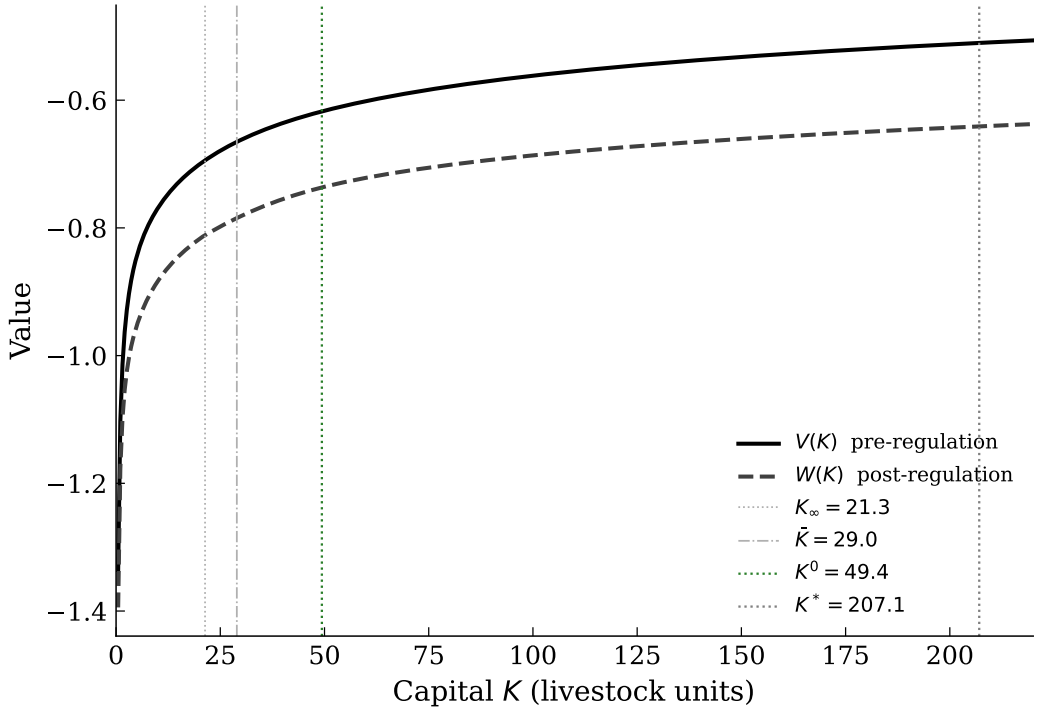

Figure 3: Pre- and post-regulation value functions

Notes: Value function iteration on a grid of 500 points. Parameters from Table 4.

Investment regions. The numerical policy function reproduces the analytical regions of Table 2. Under CRRA preferences, the upper inaction boundary shifts from the risk-neutral diagnostic $\bar{K}^{\mathrm{RN}} = 29$ to $\bar{K}^{\mathrm{CRRA}} \approx 54$, where $q(K) = \lambda p$ binds (Figure 4). At K^*, post-regulation disinvestment is -32.2 LU/yr (gross liquidation rate 15.5%).

Stranding loss by initial capital. Stranding losses are highly nonlinear in the inherited capital stock (Table 7): zero at K_∞^ϕ, EUR 272/yr at $\bar{K}^{\mathrm{RN}} = 29$, EUR 1,901/yr at the no-subsidy steady

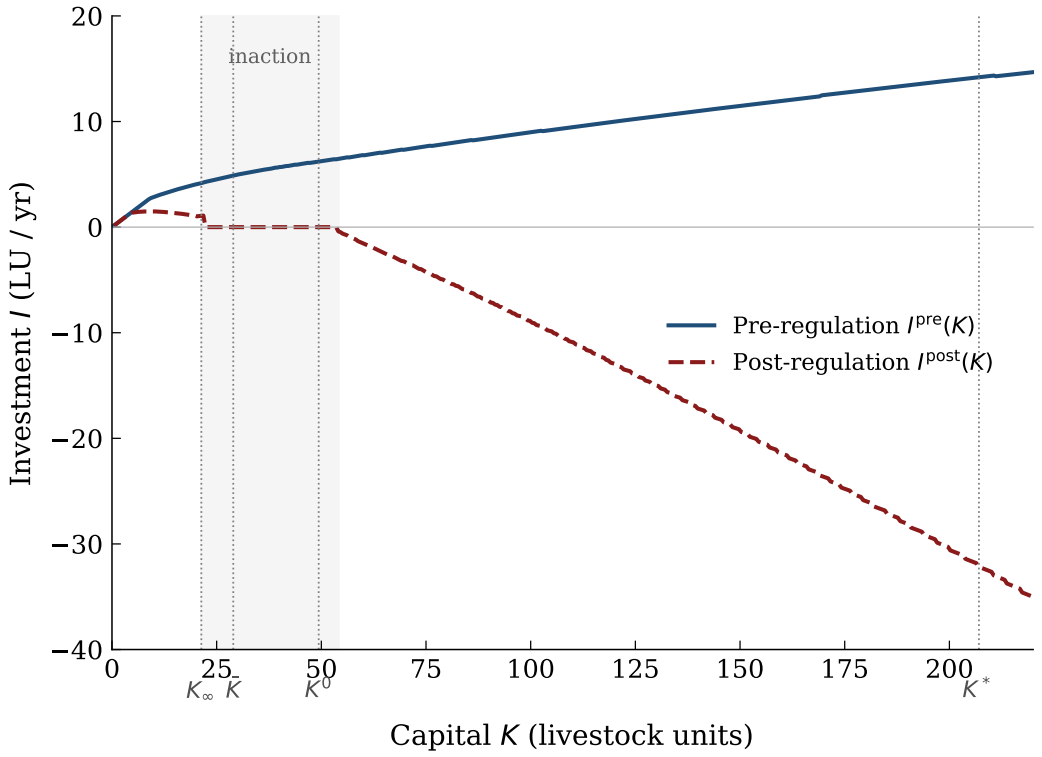

Figure 4: Optimal investment policy

Notes: Dash-dot line: analytical boundary $\bar{K}^{\mathrm{RN}} = 29.0$ under the risk-neutral benchmark. Shaded band: numerical zero-investment region under calibrated CRRA, extending to $\bar{K}^{\mathrm{CRRA}} \approx 54$; partial irreversibility ($\lambda = 0.60$) produces the discount at which the farmer prefers to hold capital rather than sell. Negative investment: disinvestment at resale price λp.

state $K^0 = 49.4$, and EUR 25,045/yr at the subsidised $K^* = 207.1$. The computed loss profile confirms the convexity predicted by Proposition 2.1 (Figure 5).

Table 7: Stranding losses by initial capital

Capital at Arrival	**LU**	**Loss (Utility)**	**CV$^{\mathrm{lin}}$ (EUR/yr)**	**Ratio to Base**
K_∞^ϕ (calibrated post-reg target)	20.7	0.000	0	0.000
$\bar{K}^{\mathrm{RN}}$ (analytical)	29.0	0.007	272	0.011
No-subsidy SS	49.4	0.050	1,901	0.076
Halfway	128.2	0.333	12,770	0.510
Subsidized SS	207.1	0.654	25,045	1.000

Notes: $\mathcal{L}$ is computed from the tangent definition in equation (1); CV$^{\mathrm{lin}}$ is the linearised money-metric of equation (39) with $c_\infty = 30{,}950$ EUR/yr. Exact CRRA equivalent loss y and compensating transfer x are in Table 8.

Amplification. The dynamic amplification multiplier is $\mathcal{M} = \mathcal{L}(K^*)/\mathcal{L}(K^{0,\mathrm{HJB}}) = 0.654/0.050 = 13.2$. It decomposes against two comparators. The static-liquidation benchmark—frictionless ad-

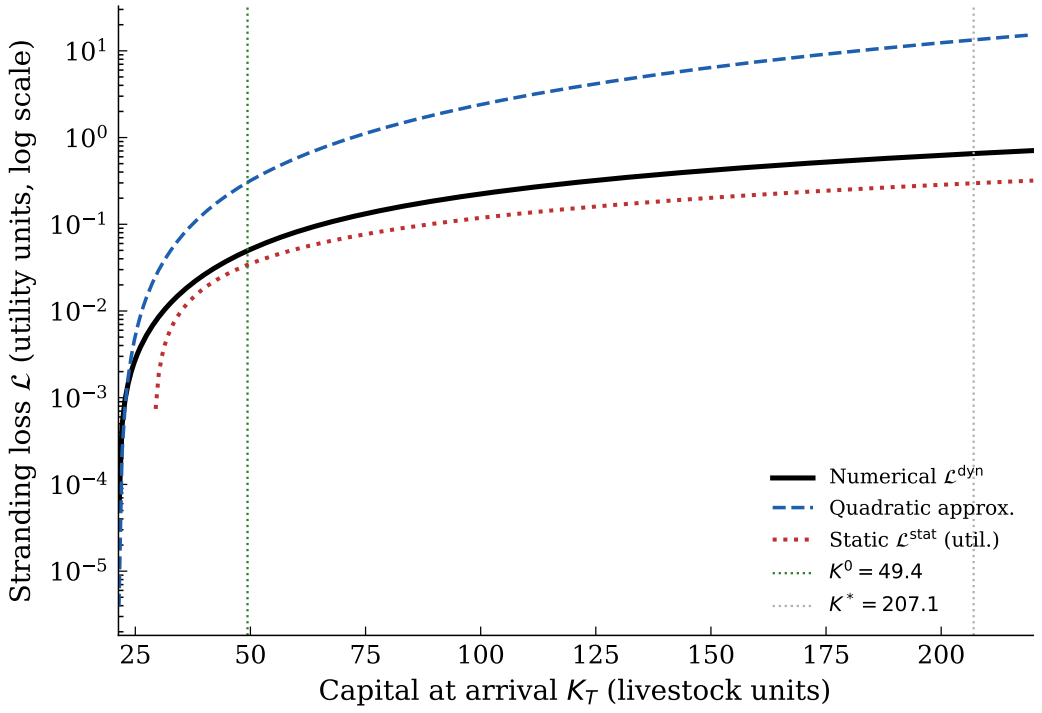

Figure 5: $\mathcal{L}(K_T)$: numerical, quadratic approximation, and static benchmark

Notes: All three curves are in utility units on a log y-axis. Solid: numerical $\mathcal{L}^{\text{dyn}}(K_T)$. Dashed: quadratic Taylor expansion at K_∞. Dotted red: static liquidation loss $(1-\lambda)p(K_T - K_\infty)^+$ from equation (11) rescaled by $u'(c_\infty)$. Vertical dotted lines mark $K^0 = 49.4$ and $K^* = 207.1$.

justment evaluated against K_∞ (Proposition 2.2)—gives $\mathcal{M}^{\text{stat}} = 6.6$; the nested frictionless limit ($\phi \to 0$) anchored at the inaction boundary $\bar{K}$ (Proposition 2.9(i)) gives 8.7. The $6.6 \to 8.7$ gap is a benchmark-anchor correction: shifting the anchor from K_∞ to $\bar{K} > K_\infty$ tightens the no-subsidy denominator $K^0 - \bar{K}$ relative to $K^* - \bar{K}$. The $8.7 \to 13.2$ gap is convex adjustment: flow costs over a protracted transition. This second gap is nearly invariant to $\pm 50\%$ perturbations in ϕ (Table 11), so the amplification reflects the *presence* of convex adjustment rather than its magnitude.

4.4 Welfare Counterfactuals

Compensating variation. Welfare is reported in three money-metric forms. The linearised index used in the climate-risk literature (Pindyck and Wang, 2013) is

$$\text{CV}^{\text{lin}} \equiv \mathcal{L}\,\frac{\rho}{u'(c_\infty)}, \tag{39}$$

the first-order annualised flow at c_∞ whose perpetual lifetime utility delivery equals $\mathcal{L}$. At baseline $\rho\,\mathcal{L}\,c_\infty \approx 0.81$, so the linearisation is no longer first-order in magnitude. Two exact CRRA objects then bracket the welfare cost: the *equivalent consumption loss* y, satisfying $u(c_\infty - y)/\rho = u(c_\infty)/\rho - \mathcal{L}$, and the *compensating transfer* x, satisfying $u(c_\infty + x)/\rho = u(c_\infty)/\rho + \mathcal{L}$. At $\gamma = 2$, $u(c) = -1/c$,

and direct inversion gives

$$y = \frac{\rho\mathcal{L}\, c_\infty^2}{1 + \rho\mathcal{L}\, c_\infty}, \qquad x = \frac{\rho\mathcal{L}\, c_\infty^2}{1 - \rho\mathcal{L}\, c_\infty}, \quad \rho\mathcal{L}\, c_\infty < 1. \tag{40}$$

The two coincide at first order ($y = x = \mathrm{CV}^{\mathrm{lin}}$ as $\rho\mathcal{L}\, c_\infty \to 0$) but separate sharply once the loss is large relative to the flow: at baseline, $y \approx$ EUR 13,845 (bounded by c_∞) while $x \approx$ EUR 131,261. The reported exact figure is the compensating transfer; the equivalent loss is the lower bound. The amplification multiplier $\mathcal{M} = 13.2$ is a ratio of utility units and is invariant to the money-metric choice.

Table 8: Money-metric welfare cost by subsidy level (EUR/farm/yr)

Scenario	**Subsidy**	K^* **(LU)**	$\mathrm{CV}^{\mathrm{lin}}$	y **(eq. loss)**	x **(comp. transfer)**
No subsidy	$s = 0.00$	49.4	1,901	1,791	2,026
Half subsidy	$s = 0.15$	87.1	6,735	5,532	8,607
Baseline CAP	$s = 0.30$	207.1	25,045	13,845	131,261

Notes: Each row re-solves the full HJB. $\mathrm{CV}^{\mathrm{lin}}$ is the linearised money-metric of equation (39); y and x are the equivalent consumption loss and the compensating transfer of equation (40). All three coincide to leading order; y and x separate sharply at baseline because $\rho\mathcal{L}\, c_\infty \approx 0.81$.

Halving the subsidy reduces all three measures by roughly three-quarters; setting it to zero removes over 90%. For a country with 5,000 dairy farms, the aggregate annual stranding cost under the status quo is EUR 125 million on the linearised measure, EUR 69 million on the equivalent-loss measure, and EUR 656 million on the compensating-transfer measure, against a direct subsidy payment of $sK^* \approx$ EUR 62,100 per farm.

Welfare ranking and zero-subsidy threshold. On the calibrated grid, the full planner objective (38) delivers $\mathcal{W}_{\mathrm{FB}} \geq \mathcal{W}_{s^*} \geq \mathcal{W}_0$, and constant-subsidy welfare crosses the no-subsidy benchmark at $\bar{s}_{\mathrm{crit}} \approx 0.12$ EUR '000/LU/yr; the baseline $s = 0.30$ sits well inside this region, so welfare rises strictly on reform (Appendix B). The welfare-maximising subsidy is zero whenever environmental damages exceed $\bar{\delta}_e \approx 0.20$ EUR '000/LU/yr — a social cost of methane of roughly €19/$\mathrm{tCO_2e}$ at the 10.4 $\mathrm{tCO_2e}$/LU/yr full life-cycle emissions factor. This threshold lies below standard social-cost-of-methane valuations under GWP_{100} conversion and is approximately at the margin under GWP_{20}.[13] The threshold $\bar{s}_{\mathrm{crit}}$ and the CV in Table 8 differ in scope: $\bar{s}_{\mathrm{crit}}$ is the planner-objective threshold over the constant-subsidy class, whereas the CV varies s along the stranding margin holding the planner objective fixed at the no-subsidy benchmark.

[13] Expressing a fixed social cost of methane SC-$\mathrm{CH_4}$ (in monetary units per tonne of $\mathrm{CH_4}$) on a per-$\mathrm{tCO_2e}$ basis divides by the GWP factor, so larger GWP gives a smaller per-$\mathrm{tCO_2e}$ number. At a US central SC-$\mathrm{CH_4}$ in the range \$1,500–1,700/$\mathrm{tCH_4}$, the per-$\mathrm{tCO_2e}$ value is ≈€52/$\mathrm{tCO_2e}$ under $\mathrm{GWP}_{100} \approx 28$ and ≈€18/$\mathrm{tCO_2e}$ under $\mathrm{GWP}_{20} \approx 84$. The €19 threshold sits well below GWP_{100} damages and approximately at GWP_{20} damages, so the zero-subsidy conclusion is robust under GWP_{100} methane valuation and near the margin under GWP_{20}.

5 Extensions and Robustness

5.1 Insurance Subsidies

Insurance subsidies operate on the same regulatory margin as direct CAP support. Denmark has no state-subsidised dairy insurance scheme, so the Danish baseline sets $s_{\text{ins}} = 0$; the counterfactual pairs a Danish-productivity dairy herd with a French-style insurance subsidy on top of CAP. France's 2023 reform (*Loi du 2 mars 2022*) provides the institutional primitives in three layers: self-insurance up to a deductible $\underline{d}$ set at 20–30% of historical revenue; subsidised private insurance on $(\underline{d}, \bar{d})$, with the state paying 70% of the premium via the Caisse Centrale de Réassurance; and a national solidarity fund covering losses above $\bar{d}$ through the Fonds National de Gestion des Risques en Agriculture.[14]

The insurance subsidy is the gap between the actuarially fair premium and the farmer's payment, scaled by pass-through:

$$s_{\text{ins}} \;=\; \psi\, \zeta\, \mathbb{E}[\lambda_a]\, D_a, \tag{41}$$

where $\mathbb{E}[\lambda_a]$ is the expected climate loss rate per unit of capital, D_a the proportional damage per event, $\zeta \in [0,1]$ the effective subsidy rate across layers, and $\psi \leq 1$ the pass-through from premium reduction to capital-cost reduction. The statutory French Layer 2 rate is $\zeta = 0.70$, rising to ≈ 0.80 including Layer 3; ψ has baseline 0.85 with sensitivity over $[0.50, 1.00]$. Enjolras and Sentis (2023) find small marginal effects of premium subsidies on take-up, bounding ψ from above. The total *effective subsidy* $s_{\text{eff}} \equiv s_{\text{CAP}} + s_{\text{ins}}$ enters the pre-regulation FOC additively,

$$\pi'(K^*_{\text{eff}}) + s_{\text{CAP}} + s_{\text{ins}} \;=\; D, \tag{42}$$

delivering $K^*_{\text{eff}} = (\alpha A/(D - s_{\text{eff}}))^{1/(1-\alpha)}$ under Cobb–Douglas. Appendix C proves that $s_{\text{ins}} > 0$ strictly raises the subsidised target, the dynamic stranding loss, and the amplification multiplier in the risk-neutral frictionless benchmark, and verifies the same monotone ranking and the *subsidy-reform complementarity* of $\mathcal{L}(K^*(s_{\text{CAP}} + s_{\text{ins}}))$ in $(s_{\text{CAP}}, s_{\text{ins}})$ numerically in the calibrated HJB at $(\phi, \gamma) = (5, 2)$.[15]

[14] The US Federal Crop Insurance Program operates analogously: premium subsidies average 62% on aggregate annual support of approximately $15 billion (USDA Risk Management Agency, 2024).

[15] The complementarity here refers to the convexity of $\mathcal{L} \circ K^*$ in the total subsidy; it is distinct from the cross-partial $\partial^2 \mathcal{L}^{11}/\partial\tau\, \partial\tau_B$ of the dynamic loss in the two regulatory *charges*, which is discussed in Appendix C.2 and can change sign under CRRA. The reform-ranking result does not require dynamic supermodularity in the charges.

Table 9: Stranding with and without insurance subsidy

	No insurance ($s = s_{\text{CAP}}$)	$\psi = 0.50$ (low pass-through)	$\psi = 0.85$ (baseline)	Δ (%) (no-ins. $\to \psi = 0.85$)
Effective subsidy (EUR '000/LU/yr)	0.300	0.316	0.327	+9.0
Subsidised target K^* (LU)	207.1	234.3	257.0	+24.1
Capital overhang $K^* - K_\infty$	185.8	213.0	235.7	+26.9
Dynamic stranding loss $\mathcal{L}$	0.654	0.767	0.863	+32.0
Linearised CV (EUR/farm)	25,045	29,401	33,052	+32.0
Amplification multiplier $\mathcal{M}$	13.2	15.5	17.4	+31.8

Notes: "$\psi = 0.85$" adds $s_{\text{ins}} = 0.027$ (equation (41)); "$\psi = 0.50$" adds $s_{\text{ins}} = 0.016$, the low-pass-through end of the sensitivity range. All columns re-solve the full HJB.

Quantitatively, adding s_{ins} to CAP raises K^* from 207 to 257 LU, the dynamic stranding loss by 32.0%, and the amplification multiplier from 13.2 to 17.4 at the baseline pass-through $\psi = 0.85$; at the low end $\psi = 0.50$ the multiplier rises only to 15.5 (Table 9). The subsidy-reform complementarity implies that removing CAP saves strictly more when insurance is also in place than when insurance has already been withdrawn, and symmetrically.

5.2 Biodiversity Regulation

Biodiversity regulation operates on a distinct externality margin: peatland restoration under the EU Nature Restoration Regulation (2024), Natura 2000 management, the 4% non-productive area requirement under CAP eco-scheme conditionality, and Denmark's 2024 Green Tripartite Agreement. The two risks target different capital profiles, so biodiversity is a second policy dimension, not a rescaling of τ. Giglio et al. (2025b,a) document that biodiversity risk is already priced in equity and CDS markets.

The farmer faces two independent one-way Poisson shocks: a carbon tax at rate $\hat{\mu}$ (charge τ, subsidy removal) and a biodiversity regulation at rate $\hat{\nu}$ (charge τ_B, subsidy removal). The regime space is $\{0,1\}^2$ with absorbing state $(1,1)$. Under frozen beliefs, risk neutrality, and the frictionless limit, the pre-regulation FOC generalises to

$$\pi'(K^{*,(2)}) + s \;=\; (\rho+\delta)p + \hat{\mu}(1-\lambda)p + \hat{\nu}(1-\lambda)p \;\equiv\; D^{(2)}, \tag{43}$$

where $\hat{\mu}(1-\lambda)p$ is the carbon-stranding premium of (28) and $\hat{\nu}(1-\lambda)p$ its biodiversity counterpart. Appendix C.2 reports the full four-regime HJB system and establishes the corresponding subsidy-reform complementarity in $(s_{\text{CAP}}, s_{\text{bio}})$.

At $\hat{\nu} = 0.10$,[16] $D^{(2)} = 0.68$ against $D = 0.52$, and the pre-regulation target falls from $K^* = 207$ to $K^{*,(2)} = 83.3$ LU — a 73% increase in the net user cost $D - s$ amplified by the Cobb–Douglas

[16] Within the Danish Green Tripartite opportunity-cost range and the Natura 2000 compliance-cost estimates of Jacobsen et al. (2019); per-hectare conversions are in the appendix.

exponent $1/(1-\alpha) = 5/3$ to a 60% reduction in capital. At current GAEC compliance the gap between full enforcement and observed enforcement acts as an implicit biodiversity subsidy of $s_{\text{bio}} \approx 0.13$. Jointly removing s_{CAP} and s_{bio} lowers the pre-regulation target to $K^{0,(2)} = 31.6$ LU and eliminates roughly 89% of the expected stranding loss. The calibrated HJB at $(\phi, \gamma) = (5, 2)$ preserves the same reform ranking: joint removal of CAP and biodiversity-enforcement support dominates sequential reform (Appendix C.2).

5.3 Parameter Sensitivity

Subsidy sensitivity. The subsidy level is the dominant determinant of stranding exposure (Table 10); Table 11 varies the remaining structural parameters.

Table 10: Stranding loss by subsidy level

Subsidy s (EUR '000/LU/yr)	K^* (LU)	$\mathcal{L}$	CV^{lin} (EUR/farm)	$\mathcal{M}$
0 (no subsidy)	49.4	0.050	1,901	1.0
0.10	70.5	0.117	4,470	2.4
0.15	87.1	0.176	6,735	3.5
0.20	110.9	0.266	10,179	5.4
0.30 (baseline CAP)	207.1	0.654	25,045	13.2

Notes: CV from equation (39). $\mathcal{M}$ uses unrounded $\mathcal{L}$. At $s = 0.40$ the analytical target exceeds 500 LU, well outside the policy-relevant range.

Table 11: Structural sensitivity: $\mathcal{L}(K^*)$ at $\pm 25\%$ and $\pm 50\%$

Parameter (baseline)	-50%	-25%	Baseline	$+25\%$	$+50\%$
Arrival rate μ (0.10)	1.643	0.999	0.654	0.447	0.315
Adjustment cost ϕ (5.0)	0.628	0.641	0.654	0.667	0.680
Tax rate τ (0.50)	0.288	0.460	0.654	0.866	1.094
Resale fraction λ (0.60)	0.236	0.385	0.654	1.248	3.027

Notes: Each row varies one parameter around its Table 4 baseline. Cells outside the standard grid ($\mu \times 0.5$ and $\lambda \times 1.5$) are solved on extended grids ($K_{\max} = 800$, $N = 600$).

Structural sensitivity. Moving from $s = 0$ to $s = 0.30$ raises $\mathcal{L}$ by a factor of 13, driven by the convexity of $K^*(s)$ near D. Among structural parameters, μ, τ, and λ each move $\mathcal{L}$ by a factor of two to twelve over the $\pm 50\%$ range — with λ generating the largest range — while ϕ moves it by under $\pm 4\%$: higher adjustment costs slow post-regulation disinvestment but also deter pre-regulation overaccumulation, and the two effects offset. The λ row inherits the U-shape of $\mathcal{M}$ around $\lambda = 0.60$: at low λ the stranding premium $\mu(1-\lambda)p$ keeps K^* near K_∞, while at high λ the frictionless comparator K^0 moves far out on the convex marginal-product curve.

Effective tax rate. At the 2035 post-deduction effective rate $\tau \approx 0.24$ (EUR 240/LU/yr), K_∞ rises to ≈ 39 LU, the overhang narrows from 186 to 168 LU, $\mathcal{L}$ falls from 0.654 to 0.275, and the CV declines to roughly EUR 18,700 per farm.

CAP pass-through. The benchmark calibration sets $\chi_s = 1$, so the entire EUR 300/LU/yr in FADN total subsidies enters the livestock-capital user cost. Most CAP income support is area-based and decoupled, so this is an upper-bound case; the pass-through into the livestock-capital composite is plausibly smaller. Table 12 reports the model at $\chi_s \in \{0.25, 0.50, 0.75, 1\}$, holding $S = 0.30$ fixed and varying $s = \chi_s S$. The amplification multiplier falls from 13.2 at $\chi_s = 1$ to roughly 1.7 at $\chi_s = 0.25$: institutional pass-through is the dominant determinant of stranding magnitudes once the carbon tax and adjustment-cost technology are fixed.

Table 12: CAP pass-through to livestock capital

Pass-through χ_s	0.25	0.50	0.75	1.00
Livestock-capital subsidy $s = \chi_s S$ (EUR '000/LU/yr)	0.075	0.150	0.225	0.300
Pre-regulation target K^* (LU)	65.6	87.1	127.6	207.1
Stranding loss $\mathcal{L}(K^*)$	0.083	0.176	0.342	0.654
Linearised CV (EUR/farm)	3,179	6,735	13,097	25,045
Amplification multiplier $\mathcal{M}$	1.7	3.5	6.9	13.2

Notes: $S = 0.30$ EUR '000/LU/yr is total CAP support per LU from FADN SE605 scaled to the 2019–2023 average milking herd; $\chi_s \in [0, 1]$ is the share capitalised into the livestock-capital composite rather than land. The $\chi_s = 0.50$ row corresponds to the half-subsidy scenario of Table 10. Each row re-solves the full HJB.

5.4 Robustness Checks

Risk aversion. Recalibrating $A(\gamma)$ at each $\gamma \in \{0.5, 1, 2, 4, 6\}$ to hold the observed exposure $K^* = 207.1$ LU fixed, the linearised CV moves within EUR 21,800–28,200 (Appendix E).

Adjustment-cost form. Under the Gomes (2001) output-scaled form $\Phi^G = (\phi_G/2)I^2/Y$ with $\phi_G \approx 2.75$ matched at the pre-regulation steady state, the amplification multiplier falls from 13.2 to 13.0 and the baseline CV from EUR 25,045 to EUR 23,680 (-5.4%). Appendix E gives the derivation.

Production technology. CES production with $\varepsilon \in [0.5, 2.0]$ shifts stranding losses by $\pm 12\%$.

Hazard process. Time-varying and regime-switching μ processes bracket the constant-μ case.

Capital risk. Stochastic shocks $\sigma \in [0, 0.08]$ amplify losses by 4–7%, second-order relative to the subsidy channel. Appendix E reports the full grid.

Partial subsidy persistence. The baseline assumes full subsidy removal at policy arrival ($s_r = 0$). Table 13 re-solves for $s_r \in \{0, 0.10, 0.15, 0.30\}$, holding all other parameters at baseline.

Table 13: Stranding losses under partial subsidy persistence

s_r (EUR '000/LU/yr)	$\tau_{\text{eff}} = \tau - s_r$	K_∞^ϕ (LU)	$\mathcal{L}$	CV^{lin} (EUR)
0.00 (baseline)	0.50	20.7	0.654	25,045
0.10	0.40	25.3	0.497	23,098
0.15	0.35	28.4	0.423	21,918
0.30 (CAP persists)	0.20	41.7	0.227	17,258

Notes: $K^* = 207$ LU in all rows. Each entry re-solves the post-regulation HJB at effective tax $\tau_{\text{eff}} = \tau - s_r$.

Even at $s_r = s$, the carbon tax alone generates stranding losses worth roughly two-thirds of the baseline CV, because the tax shifts K_∞ well below K^*; full bundling ($s_r = 0$) raises the CV by roughly 50% relative to the tax-only case.

6 Conclusion

Climate-transition and biodiversity-regulation risks convert agricultural subsidies into a stranded-capital problem. Strict convexity of the stranding loss in the capital overhang means welfare costs grow more than proportionally with excess capital, and convex adjustment costs amplify this static measure by a factor of two because accumulated capital cannot be liquidated instantaneously. Insurance subsidies and direct payments feed the same overhang through the user-cost wedge; risk aversion adds a separate channel, raising the pre-regulation capital target through the marginal-utility valuation of post-arrival resale proceeds. Under two independent policy shocks, the composite loss is strictly supermodular in the subsidy pair in the risk-neutral frictionless benchmark. In the calibrated HJB the same joint-reform ranking holds numerically. The biodiversity and insurance exercises should therefore be interpreted as evidence that the overhang channel is not specific to direct payments, rather than as a general theorem on supermodularity of regulatory losses.

The welfare-maximising CAP subsidy is zero at damage levels below standard methane valuations under GWP_{100} conversion and close to the corresponding GWP_{20} valuation. The marginal return to reform is increasing in the inherited subsidy distortion: economies that have accumulated the largest agricultural overhangs face the steepest welfare losses from delay. Joint removal of direct payments and insurance support dominates sequential reform, and the same logic extends pairwise to direct payments and biodiversity-enforcement support; the three-instrument generalisation follows the same logic but is not formally proven.

Several generalisations preserve the mechanism. Heterogeneous farms amplify aggregate stranding: Jensen's inequality applied to the convex loss implies that the average loss across farms exceeds the loss at the average farm, so the representative-agent estimates are conservative provided the overhang distribution lies in the post-regulation overhang region and subsidy capitalisation is uniform across farm types. A disagreement framework over policy timing (Baldauf et al., 2020;

Bakkensen et al., 2025) amplifies aggregate losses through the same channel. Interacting climate-driven capital losses with financial frictions or sovereign default risk (Phan and Schwartzman, 2024) would slow recovery further.

The model is partial equilibrium. For Denmark, where agricultural capital is a small share of total private capital, general-equilibrium rental-rate effects are negligible; for larger agricultural economies such as France, factor-price responses would attenuate the stranding losses. The calibration relies on aggregate Danish dairy moments rather than farm-level distributions, so the cross-sectional predictions of the heterogeneous-farm extension cannot yet be tested.

The framework integrates physical and transition risk in a single capital-accumulation problem: physical risk enters as a Brownian disturbance to capital, transition risk as a Poisson regime switch that delivers the carbon tax and the biodiversity-enforcement charge. The two channels are independent in the baseline; a richer specification in which climate change accelerates biological catastrophes — mass mortality, novel pathogens — would couple them.

The anticipatory-inaction time of Appendix A.2 predicts step-wise contraction of agricultural investment at salient policy signals — the 2020 Danish Climate Act, the 2022 Green Tax Reform, the 2024 Tripartite Agreement — rather than a single contraction at enactment. Farm-level investment microdata around these dates would discriminate the learning-augmented realised loss from the body's static benchmark and identify the speed of belief updating from observed timing rather than from cross-sectional moments. Belief heterogeneity between farmers and policymakers about the timing of climate and biodiversity regulation, and whether pre-announcement signals coordinate expectations enough to shrink inherited overhang, would discipline the disagreement framework. Cross-country quantification of the stranding multiplier across the EU27 — where the share of agricultural capital, the depth of CAP support, and the political feasibility of carbon pricing vary widely — extends the exercise of Appendix D to the full union.

Code and Data Availability

A replication package containing the HJB solver, calibration files, and counterfactual scripts that reproduce all numerical results, figures, and tables in the paper is available at the following repository: Dropbox replication package.

References

Andrew B. Abel and Janice C. Eberly. Optimal investment with costly reversibility. *Review of Economic Studies*, 63(4):581–593, 1996.

Yves Achdou, Jiequn Han, Jean-Michel Lasry, Pierre-Louis Lions, and Benjamin Moll. Income and wealth distribution in macroeconomics: A continuous-time approach. *Review of Economic Studies*, 89(1):45–86, 2022.

Francis Annan and Wolfram Schlenker. Federal crop insurance and the disincentive to adapt to extreme heat. *American Economic Review*, 105(5):262–266, 2015.

Laura A. Bakkensen, Toan Phan, and Russell Wong. Leveraging the disagreement on climate change: Theory and evidence. *Journal of Political Economy*, 133(10):3132–3166, 2025.

Markus Baldauf, Lorenzo Garlappi, and Constantine Yannelis. Does climate change affect real estate prices? Only if you believe in it. *Review of Financial Studies*, 33(3):1256–1295, 2020.

Michael Barnett. Climate change and uncertainty: An asset pricing perspective. *Management Science*, 69(12):7562–7584, 2023.

Nicholas Bloom. The impact of uncertainty shocks. *Econometrica*, 77(3):623–685, 2009.

Patrick Bolton and Marcin Kacperczyk. Do investors care about carbon risk? *Journal of Financial Economics*, 142(2):517–549, 2021.

Emanuele Campiglio, Louis Daumas, Pierre Monnin, and Adrian von Jagow. Climate-related risks in financial assets. *Journal of Economic Surveys*, 37(3):950–992, 2023.

Pavel Ciaian and d'Artis Kancs. The capitalisation of area payments into farmland rents: Micro evidence from the new EU member states. *Canadian Journal of Agricultural Economics*, 60(4): 517–540, 2012.

Danish Ministry of Taxation. Agreement on a Green Denmark: Carbon tax on agriculture, 2024. Legislative agreement, June 2024.

Avinash K. Dixit and Robert S. Pindyck. *Investment Under Uncertainty*. Princeton University Press, 1994.

Geoffroy Enjolras and Patrick Sentis. Crop insurance take-up and premium subsidies: Evidence from france. *Working paper (Banque de France / CEP)*, 2023.

European Commission. The common agricultural policy at a glance: Budget and implementation, 2021–2027. Directorate-General for Agriculture and Rural Development, 2024. Available at https://agriculture.ec.europa.eu/common-agricultural-policy/cap-overview_en.

European Environment Agency. Annual european Union greenhouse gas inventory 1990–2022 and inventory report 2024. Technical Report EEA Report 04/2024, European Environment Agency, Copenhagen, 2024.

European Union. Regulation (eu) 2024/1991 of the european parliament and of the council of 24 june 2024 on nature restoration and amending regulation (eu) 2022/869. Official Journal of the European Union, L series, 29 July 2024, 2024. Available at https://eur-lex.europa.eu/eli/reg/2024/1991.

Wendell H. Fleming and H. Mete Soner. *Controlled Markov Processes and Viscosity Solutions*. Springer, 2nd edition, 2006.

Stefano Giglio, Theresa Kuchler, Johannes Stroebel, and Olivier Wang. The economics of biodiversity loss. Working Paper, 2025a.

Stefano Giglio, Theresa Kuchler, Johannes Stroebel, and Xuran Zeng. Biodiversity risk. *Review of Finance*, 2025b. forthcoming.

João F. Gomes. Financing investment. *American Economic Review*, 91(5):1263–1285, 2001.

Zvi Griliches. The sources of measured productivity growth: United States agriculture, 1940–60. *Journal of Political Economy*, 71(4):331–346, 1963.

Christoph Hambel and Frederick van der Ploeg. Policy transition risk, carbon premiums, and asset prices. *Journal of Monetary Economics*, 152:103780, 2025.

Kevin A. Hassett and Gilbert E. Metcalf. Investment with uncertain tax policy: Does random tax policy discourage investment? *Economic Journal*, 109(457):372–393, 1999.

Nathan P. Hendricks, Joseph P. Janzen, and Aaron Smith. The effects of policy expectations on crop supply, with an application to base updating. *American Journal of Agricultural Economics*, 96(3):903–923, 2014.

James R. Hines. Three sides of Harberger triangles. *Journal of Economic Perspectives*, 13(2): 167–188, 1999.

Harrison Hong, Neng Wang, and Jinqiang Yang. Welfare consequences of sustainable finance. *Review of Financial Studies*, 36(12):4864–4918, 2023.

Brian H. Jacobsen, Uwe Latacz-Lohmann, Harry Luesink, Rolf Michels, and Bernhard Osterburg. Costs of regulating ammonia emissions from livestock farms near Natura 2000 areas—analyses of case farms from Germany, Netherlands and Denmark. *Journal of Environmental Management*, 246:897–908, 2019.

Hee Soo Kim, Christian Matthes, and Toan Phan. Severe weather and the macroeconomy. *American Economic Journal: Macroeconomics*, 17(2):315–341, 2025.

Barrett E. Kirwan. The incidence of U.S. agricultural subsidies on farmland rental rates. *Journal of Political Economy*, 117(1):138–164, 2009.

Adriaan J. Kortleve et al. Stranded assets in European agriculture during food system transformations. *Nature Food*, 2025. doi: 10.1038/s43016-025-01283-z. Full author list and volume/pages to be verified against the published version.

Christophe McGlade and Paul Ekins. The geographical distribution of fossil fuels unused when limiting global warming to 2°C. *Nature*, 517(7533):187–190, 2015.

Yair Mundlak. Production and supply. *Handbook of Agricultural Economics*, 1:3–85, 2001.

Ľuboš Pástor and Pietro Veronesi. Uncertainty about government policy and stock prices. *Journal of Finance*, 67(4):1219–1264, 2012.

Ľuboš Pástor and Pietro Veronesi. Political uncertainty and risk premia. *Journal of Financial Economics*, 110(3):520–545, 2013.

Toan Phan. Climate risks in financial markets. In *Handbook of the Economics of Climate Change, Volume 2*. Elsevier, 2026. Forthcoming.

Toan Phan and Felipe Schwartzman. Climate defaults and financial adaptation. *European Economic Review*, 170:104866, 2024.

Robert S. Pindyck. Irreversible investment, capacity choice, and the value of the firm. *American Economic Review*, 78(5):969–985, 1988.

Robert S. Pindyck and Neng Wang. The economic and policy consequences of catastrophes. *American Economic Journal: Economic Policy*, 5(4):306–339, 2013. doi: 10.1257/pol.5.4.306.

Julie Rozenberg, Adrien Vogt-Schilb, and Stéphane Hallegatte. Instrument choice and stranded assets in the transition to clean capital. *Journal of Environmental Economics and Management*, 100:102183, 2020.

USDA Economic Research Service. Farm sector income and finances: Farm business financial ratios. Technical report, U.S. Department of Agriculture, 2020. Discount rates for agricultural capital typically range from 3–5%.

USDA Risk Management Agency. Federal crop insurance program premium subsidy rates and aggregate liability statistics. U.S. Department of Agriculture, 2024. Premium subsidies average 62% across plans; aggregate annual subsidy approximately $15 billion.

Frederick van der Ploeg and Armon Rezai. The risk of policy tipping and stranded carbon assets. *Journal of Environmental Economics and Management*, 100:102258, 2020.

Dan Welsby, James Price, Steve Pye, and Paul Ekins. Unextractable fossil fuels in a 1.5°C world. *Nature*, 597(7875):230–234, 2021.

Appendix

A Learning

Two dimensions of the policy are unobserved: the arrival intensity μ and the severity τ. Conjugate filters deliver tractable posteriors on each, and the full belief state admits a certainty-equivalence reduction to the baseline HJB at second order in posterior dispersion.

A.1 Timing Risk

Two distinct Poisson processes share the common rate μ: an *observable* signal process generating legislative announcements and commission reports, and an unobservable terminal process whose first arrival enacts the tax. Signals and the terminal event are conditionally independent given μ, so the information content of signals is purely inferential—they update $\hat{\mu}$ but do not themselves trigger the tax. The farmer holds a Gamma prior $\mu \sim \text{Gamma}(\alpha_0, \beta_0)$ with mean $\hat{\mu}_0 = \alpha_0/\beta_0$. The Gamma–Poisson conjugacy ensures tractable updating: after observing the signal process for t years with n realised signals, the posterior is $\text{Gamma}(\alpha_0 + n,\, \beta_0 + t)$ with mean

$$\hat{\mu}_{n,t} \;=\; \frac{\alpha_0 + n}{\beta_0 + t}.$$

Proposition A.1. *Under Gamma–Poisson updating with prior* $\text{Gamma}(\alpha_0, \beta_0)$ *and Cobb–Douglas production:*

$$\hat{\mu}_{n,t} = \frac{\alpha_0 + n}{\beta_0 + t}, \qquad \frac{\partial K^*}{\partial \hat{\mu}} < 0, \qquad \frac{\partial K^*}{\partial n} < 0.$$

Two forces on beliefs. The *absence* of a policy arrival lowers $\hat{\mu}$ continuously (as $\beta_0 + t$ drifts up with n fixed), encouraging capital accumulation: longer periods without regulation make the farmer more optimistic. A *discrete arrival signal*—a legislative announcement that increments n—raises $\hat{\mu}$ discontinuously, triggering pre-emptive disinvestment.

The learning channel interacts with the subsidy amplification mechanism: higher $\hat{\mu}$ reduces K^* through the user-cost channel (D increases in μ), which compresses the capital overhang $K^* - K_\infty$ and attenuates stranding losses. Bayesian learning compresses the overhang pre-emptively, provided signals arrive sufficiently early.

Table 14: Danish policy signals and Gamma–Poisson posterior

Date	**Signal**	n	α_n	β_t	$\hat{\mu}_{n,t}$
Pre-2020	Prior	0	2	20.0	0.100
Jun 2020	Climate Act (70% target)	1	3	20.5	0.146
Oct 2021	Ag. agreement (55–65% target)	2	4	21.8	0.183
Jun 2022	Green Tax Reform; Expert Comm.	3	5	22.5	0.222
Feb 2024	Expert report (ag. CO_2e tax)	4	6	24.2	0.248
Jun 2024	Green Tripartite (DKK 300–750)	5	7	24.5	0.286

Notes: t in years from January 2020. The November 2024 enactment resolves the Poisson uncertainty; the deterministic-delay regime begins, with effective taxation from January 2030.

Calibrated signals. The posterior mean rises from 0.10 to 0.29 across the five-signal sequence; at the terminal posterior $\hat{\mu} = 0.286$, the implied target falls to $K^* \approx 47$ LU because the stranding premium $\hat{\mu}(1-\lambda)p = 0.46$ raises D from 0.52 to 0.82.

Proof. The posterior mean follows from Gamma–Poisson conjugacy. For the monotonicity results, substitute $\hat{\mu}_{n,t}$ into the pre-regulation first-order condition $\alpha A(K^*)^{\alpha-1} = D(\hat{\mu}) - s$ where $D(\hat{\mu}) = (\rho+\delta)p + \hat{\mu}(1-\lambda)p$. Since D is increasing in $\hat{\mu}$ and the marginal product is decreasing in K, the implicit-function theorem gives $\partial K^*/\partial\hat{\mu} < 0$. Since $\hat{\mu}_{n,t}$ is increasing in n, $\partial K^*/\partial n < 0$ follows. □

A.2 Anticipatory Inaction

The pre-regulation user cost rises with the posterior $\hat{\mu}_t$, so the boundaries of the pre-regulation policy regions of §2.4 move over time even before the regulation arrives. The farmer therefore switches from accumulation to inaction strictly before enactment, at the *anticipatory inaction time*.

Definition. Let $V(K;\hat{\mu})$ denote the pre-regulation value function at posterior $\hat{\mu}$, and let $\bar{K}^{\text{pre}}(\hat{\mu})$ denote the upper edge of the pre-regulation inaction band — the largest K at which the pre-regulation shadow value $V'(K;\hat{\mu})/u'(c)$ equals the resale price λp. By the user-cost channel of Proposition A.1, $\bar{K}^{\text{pre}}$ is strictly decreasing in $\hat{\mu}$, with $\bar{K}^{\text{pre}}(\hat{\mu}) > K^*(\hat{\mu})$ at every $\hat{\mu}$. The anticipatory inaction time is

$$T^* \equiv \inf\{t \geq 0 : K_t \geq \bar{K}^{\text{pre}}(\hat{\mu}_t)\}. \tag{44}$$

For $t < T^*$, K_t lies below the disinvestment threshold of the current posterior and the farmer accumulates toward $K^*(\hat{\mu}_t)$. At T^*, signals have pushed the threshold below her stock; she enters the inaction band, and if $\hat{\mu}_t$ continues to rise she crosses into the disinvestment region.

Structural parallel. The construction is the time-domain counterpart of the state-domain kinked-cost crossing of §2.4. Standard irreversible-investment problems with kinked adjustment costs (Dixit and Pindyck, 1994; Pindyck, 1988; Abel and Eberly, 1996) feature a shadow value crossing

the kink as exogenous primitives shift. Here the shift is driven by belief revision rather than by primitive variation, and the crossing direction is reversed: the farmer moves from active investment to inaction as $\hat{\mu}_t$ rises with successive signals.

Calibration. The 2020–2024 Danish signal sequence (Table 14) raises $\hat{\mu}_t$ from 0.10 to 0.286 and contracts $K^*(\hat{\mu}_t)$ from 207 LU to approximately 47 LU. Anchoring the farmer at $K_0 = 207$ LU in early 2020, the first signal — the June 2020 Climate Act — lowers $\bar{K}^{\text{pre}}(\hat{\mu}_t)$ below the anchor stock, so T^* effectively coincides with the first signal date. The farmer remains in the pre-regulation disinvestment region for the rest of the window, contracting toward the moving target until the November 2024 enactment freezes the posterior; her realised stock at enactment is strictly below the static benchmark.

Empirical implication. Anticipatory contraction trims the overhang the farmer carries into reform. The body's stranding magnitudes are evaluated at the 2019 anchor $K^* = 207$ LU and correspond to a no-learning counterfactual; under signal-driven learning, the realised stock at enactment is strictly lower and the realised loss is correspondingly smaller. The model therefore predicts step-wise contraction of agricultural investment at salient signals — the 2020 Climate Act, the 2022 Green Tax Reform, the 2024 Tripartite Agreement — rather than a single contraction at enactment, an empirical signature distinct from the cross-sectional amplification multipliers in the body. The decomposition of realised stranding losses into anticipatory and ex-post components, and the formal characterisation of T^* at general signal sequences, are the subject of future work.

A.3 Severity

The baseline model treats τ as known. Joint uncertainty over timing and severity has prior variance $\sigma^2_{\tau,0}$ on the tax level, distinct from the capital-diffusion volatility σ used elsewhere; all results nest the baseline as the special case $\sigma^2_{\tau,0} \to 0$. The same formal apparatus applies to uncertainty over the net policy shock $\Delta = \tau + (s - s_r)$ rather than τ in isolation: under institutional separation, the residual subsidy s_r is itself drawn at the regime switch, and the variance of Δ inherits both the variance of τ and the variance of s_r.

Assumption 1. The farmer does not observe μ or τ directly. There are two distinct sources of uncertainty.

Timing uncertainty. As in the baseline: $\mu \sim \Gamma(\alpha_0, \beta_0)$, posterior under non-arrival $\hat{\mu}_t = \alpha_0/(\beta_0+t)$, and signals increment $\alpha_n = \alpha_0 + n$.

Severity uncertainty. Conditional on eventual arrival, the tax level τ is unknown with prior $\tau \sim N(\bar{\tau}_0, \sigma^2_{\tau,0})$. The farmer observes noisy policy signals $z_j = \tau + \varepsilon_j$, $\varepsilon_j \sim N(0, \sigma^2_z)$, independently across j. After m signals:

$$\tau \mid z_{1:m} \sim N(\bar{\tau}_m, \sigma^2_{\tau,m}), \qquad \sigma^{-2}_{\tau,m} = \sigma^{-2}_{\tau,0} + m\sigma^{-2}_z.$$

Each signal updates $\bar{\tau}_m$ toward the true level and reduces posterior variance.

Belief state. Between tax-severity signals, the sufficient statistics for beliefs are $\boldsymbol{\theta}_t = (\alpha_0, \beta_0 + t, \bar{\tau}_m, \sigma^2_{\tau,m})$. The only continuous movement between signals is the deterministic drift of the rate parameter from β_0 to $\beta_0 + t$.

Denmark's 2024 agreement set the initial rate at DKK 300/tCO_2e from 2030, rising to DKK 750 by 2035, but the legislation includes a review clause that allows Parliament to revise both the level and the escalation path. The EU's proposed Agricultural Emissions Trading System remains under negotiation, with permit-price projections ranging from EUR 30 to EUR 150/tCO_2e depending on the cap trajectory.

The pre-regulation value function becomes $V(K, \boldsymbol{\theta})$, with HJB generalising (27) to

$$(\rho+\hat{\mu})V(K,\boldsymbol{\theta}) = \max_I \Big\{ u\big(\pi(K)+sK-C(I,K)\big) + V_K(I-\delta K) + \tfrac{1}{2}\sigma^2 K^2 V_{KK} + V_\beta + \hat{\mu}\,\mathbb{E}_\tau[W(K;\tau)] \Big\}. \tag{45}$$

Certainty-equivalence reduction.

Proposition A.2. *Fix a posterior with mean $\bar{\boldsymbol{\theta}}$ and define $\hat{V}(K) \equiv V(K;\bar{\boldsymbol{\theta}})$. If $\boldsymbol{\theta} \mapsto V(K;\boldsymbol{\theta})$ is C^2 on a compact neighborhood Θ of $\bar{\boldsymbol{\theta}}$, then*

$$\big|\mathbb{E}[V(K;\boldsymbol{\theta})] - \hat{V}(K)\big| \;\le\; \frac{1}{2} \sup_{\tilde{\boldsymbol{\theta}}\in\Theta} \big\| D^2_{\boldsymbol{\theta}} V(K;\tilde{\boldsymbol{\theta}}) \big\| \;\cdot\; \mathbb{E}\big[\|\boldsymbol{\theta} - \bar{\boldsymbol{\theta}}\|^2\big]. \tag{46}$$

The error is second order in posterior dispersion.

Proof. Fix K. By Taylor's theorem, for each realization of $\boldsymbol{\theta}$ there exists a point $\tilde{\boldsymbol{\theta}}$ on the line segment between $\boldsymbol{\theta}$ and $\bar{\boldsymbol{\theta}}$ such that

$$V(K;\boldsymbol{\theta}) = V(K;\bar{\boldsymbol{\theta}}) + D_{\boldsymbol{\theta}} V(K;\bar{\boldsymbol{\theta}}) \cdot (\boldsymbol{\theta} - \bar{\boldsymbol{\theta}}) + \tfrac{1}{2}\,(\boldsymbol{\theta} - \bar{\boldsymbol{\theta}})^\top D^2_{\boldsymbol{\theta}} V(K;\tilde{\boldsymbol{\theta}})\,(\boldsymbol{\theta} - \bar{\boldsymbol{\theta}}).$$

Take expectations. Since $\bar{\boldsymbol{\theta}} = \mathbb{E}[\boldsymbol{\theta}]$, the linear term vanishes. Using the operator-norm bound $|x^\top A x| \le \|A\|\,\|x\|^2$ on the quadratic remainder gives (46). □

Remark A.3. At calibrated parameters, the relative CE error is $< 0.02\%$ for μ-learning and $< 0.9\%$ for τ-learning; after three severity signals it contracts to 0.3%.

Severity-signal response.

Proposition A.4. *Fix K_T and define the local quadratic approximation*

$$\widetilde{\mathcal{L}}(K_T;\tau) \equiv \tfrac{1}{2}\,|W''(K_\infty(\tau))|\big(K_T - K_\infty(\tau)\big)^2. \tag{47}$$

Assume $\widetilde{\mathcal{L}}_{\tau\tau}(K_T;\bar{\tau}) > 0$. Then

$$\mathbb{E}_\tau[\widetilde{\mathcal{L}}(K_T;\tau)] = \widetilde{\mathcal{L}}(K_T;\bar{\tau}) + \tfrac{1}{2}\,\widetilde{\mathcal{L}}_{\tau\tau}(K_T;\bar{\tau})\,\mathrm{Var}(\tau) + o\big(\mathrm{Var}(\tau)\big). \tag{48}$$

The assumption holds for K_T sufficiently close to $K_\infty(\bar{\tau})$; whether it holds at the calibrated $K_T = K^* \gg K_\infty(\bar{\tau})$ is verified numerically in Remark A.5.

Proof. Define $h(\tau) \equiv \widetilde{\mathcal{L}}(K_T;\tau)$. A second-order Taylor expansion around $\bar{\tau}$ gives $h(\tau) = h(\bar{\tau}) + h'(\bar{\tau})(\tau-\bar{\tau}) + \frac{1}{2}h''(\bar{\tau})(\tau-\bar{\tau})^2 + r(\tau)$ with $\mathbb{E}[r(\tau)] = o(\mathrm{Var}(\tau))$. Taking expectations and using $\mathbb{E}[\tau-\bar{\tau}] = 0$ yields (48).

For the local claim, expand $|W''(K_\infty(\tau))|$ and $(K_T - K_\infty(\tau))^2$ around $\bar{\tau}$. A sufficient condition for $\widetilde{\mathcal{L}}_{\tau\tau}(K_T;\bar{\tau}) > 0$ in the linear-quadratic regime is $(K'_\infty)^2 > (K_T - K_\infty)\,K''_\infty$; under Cobb–Douglas with $\nu \equiv 1/(1-\alpha)$ this reduces to $K_\infty(\bar{\tau}) > [(\nu+1)/(2\nu+1)]\,K_T$. At calibrated $\alpha = 0.40$ the threshold is $K_\infty > (8/13)\,K_T$, which fails at $(K^*, K_\infty) = (207.1, 21.3)$ LU; Remark A.5 verifies positivity numerically at this calibration. □

Remark A.5. A finite-difference evaluation of $\widetilde{\mathcal{L}}(K^*;\tau)$ on a grid $\tau \in [0.40, 0.60]$ confirms that the map is strictly convex in τ at the calibrated $K_T = K^* = 207.1$ LU: the numerical second derivative is strictly positive throughout the grid, so the variance term in (48) enters with a positive coefficient despite the analytical sufficient condition failing.

Severity-signal scenario. At $t = 3$, a signal $z_1 = 0.70$ raises the posterior tax mean from $\bar{\tau} = 0.50$ to 0.557 under Normal updating. The post-regulation steady state falls from $K_\infty = 21.3$ to 19.1 LU, and $\mathcal{L}(K^*)$ rises by 2.4%. Severity uncertainty contributes much less to stranding risk than timing uncertainty across the sensitivity grid. Magnitude uncertainty moves $K_\infty \approx 21$ LU: large percentage changes in τ yield small absolute changes in the overhang $K^* - K_\infty$. Timing uncertainty moves $K_T \approx 207$ LU, and the convexity of $\mathcal{L}$ amplifies the resulting swings. Where τ-uncertainty dominates—K^* close to K_∞—stranding is not first-order. The calibration parameters are $\bar{\tau}_0 = 0.50$, $\sigma^2_{\tau,0} = 0.04$, $\sigma^2_z = 0.10$.

B Proofs

Assumption 2 (Post-regulation concavity)**.** The post-regulation value function W is C^2 and strictly concave on the relevant overhang interval $(0, \bar{K})$ for $\phi > 0$. In the frictionless limit $\phi = 0$ with $\lambda < 1$, W is C^2 and strictly concave on $(0, \bar{K})$ and linear at slope λp on $(\bar{K}, \infty)$.

Discussion of Assumption 2. The HJB maximand

$$u\big(\pi(K) - \tau_{\text{eff}}K - C(I,K)\big) + W'(K)(I - \delta K) + \tfrac{1}{2}\sigma^2 K^2\, W''(K)$$

combines a strictly concave utility, a strictly concave production technology, and a cost $C(I,K) = \tilde{p}(I)I + (\phi/2)I^2/K$ strictly convex in I for $\phi > 0$ (the kink term $\tilde{p}(I)I$ is piecewise linear with $p > \lambda p$, hence convex; the quadratic component is strictly convex). Under classical regularity (Fleming and Soner, 2006) the dynamic-programming operator maps concave functions to concave functions, providing analytical support for the assumption in the deterministic risk-neutral benchmark, where $u' \equiv 1$ and the HJB reduces to a standard concave-control problem. Under CRRA and stochastic $\sigma > 0$ a fully rigorous proof would require a verification theorem; the numerical solution on the calibrated grid satisfies $W''(K) < 0$ at every grid point, with the sign preserved under grid doubling.

In the frictionless limit, instantaneous liquidation at the resale price gives $W(K) = W(\bar{K}) + \lambda p(K - \bar{K})$ for $K > \bar{K}$, so $W'' \equiv 0$ on $(\bar{K}, \infty)$ and concavity holds only weakly there.

Proof of Lemma 2.5. Under the maintained Cobb–Douglas technology, $\pi(K)/K = AK^{\alpha-1} \to 0$ for $\alpha \in (0, 1)$. More generally, under the upper Inada condition $\pi'(K) \to 0$ with $\pi \in C^1$, for any fixed $K_0 > 0$,

$$\frac{\pi(K)}{K} = \frac{\pi(K_0)}{K} + \frac{1}{K}\int_{K_0}^{K} \pi'(z)\,\mathrm{d}z \to 0$$

by Cesàro averaging. Therefore, with $\tau_{\text{eff}} > 0$, there exists $K_1 > 0$ with $\pi(K) - \tau_{\text{eff}} K < 0$ for all $K \geq K_1$. For every $I \geq 0$, $C(I, K) = pI + (\phi/2)I^2/K \geq 0$, so for $K \geq K_1$ and $I \geq 0$,

$$c^1(K, I) = \pi(K) - \tau_{\text{eff}} K - C(I, K) \leq \pi(K) - \tau_{\text{eff}} K < 0.$$

Admissibility requires $c^1 > 0$, so no admissible optimum has $I^*(K) \geq 0$ on the upper tail.

For the candidate $I = -aK$ with a as in (23),

$$c^1(K, -aK) = \pi(K) + K\Big(\lambda p\, a - \frac{\phi}{2}a^2 - \tau_{\text{eff}}\Big),$$

and the bracketed coefficient is strictly positive, so there exists $K_2 \geq K_1$ with $c^1(K, -aK) > 0$ for all $K \geq K_2$. Hence every admissible optimum satisfies $I^*(K) < 0$ for all sufficiently large K.

On the disinvestment branch, $C_I(I, K) = \lambda p + \phi I/K$, and the first-order condition gives $q(K) = \lambda p + \phi I^*(K)/K < \lambda p$ whenever $I^*(K) < 0$. Thus there exists $K_H > K_\infty$ with $q(K_H) < \lambda p$, while $q(K_\infty) = p + \phi\delta > \lambda p$. Set $\bar{K} \equiv \inf\{K > K_\infty : q(K) = \lambda p\}$; by continuity of q and $q(K_\infty) > \lambda p > q(K_H)$, the intermediate value theorem yields $\bar{K} \in (K_\infty, K_H]$ with $q(\bar{K}) = \lambda p$.

On $[K_\infty, \bar{K}]$, $q(K_\infty) - p = \phi\delta > 0$ and $q(\bar{K}) - p = -(1 - \lambda)p < 0$. The intermediate value theorem yields $K_p \in (K_\infty, \bar{K})$ with $q(K_p) = p$. □

Proof of Lemma 2.6. Part (i). Let $r(K) \equiv I^*(K)/K$ and $G(K) \equiv K(r(K) - \delta)$. Since $I^*(K_\infty) = \delta K_\infty$, $r(K_\infty) = \delta$, and

$$G'(K) = r(K) - \delta + Kr'(K), \qquad G'(K_\infty) = K_\infty r'(K_\infty).$$

Local asymptotic stability is equivalent to $G'(K_\infty) < 0$, hence to $r'(K_\infty) < 0$ since $K_\infty > 0$. Because $q(K_\infty) = p + \phi\delta > p$, the policy lies on the positive-investment branch in a neighbourhood of K_∞, on which the first-order condition gives $q(K) = p + \phi r(K)$ and therefore

$$q'(K) = \phi r'(K). \tag{49}$$

Thus $q'(K_\infty) = \phi r'(K_\infty) < 0$. By continuity of r', $q' < 0$ on a neighbourhood U of K_∞. On U, q is strictly decreasing, hence injective; $\{K \in U : q(K) = y\}$ is a singleton for every $y \in q(U)$.

Part (ii). Single-crossing at p gives $\#\{K \geq K_\infty : q(K) = p\} \leq 1$; with existence in Lemma 2.5, K_p is unique. The same argument at λp gives uniqueness of $\bar{K}$.

At $\gamma = 0$ and $\sigma = 0$, $u' \equiv 1$, so $q = W'$ and (25) reduces to $q'(K) = W''(K)$. Assumption 2 gives $W''(K) < 0$ on the overhang interval, so q is strictly decreasing there and single-crosses both p and λp.

□

Remark B.1. (i) Under calibrated CRRA preferences, the second term in (25) can be positive on the investment branch, so concavity of W alone does not yield $q' < 0$. Single crossing is verified directly on the finite-difference solution: $\max_i (q_{i+1} - q_i)/(K_{i+1} - K_i) < 0$, with the sign preserved under grid doubling from $N = 500$ to $N = 1000$, and monotone PCHIP interpolation preserves the ordering between nodes.

(ii) The tail-feasibility condition (23) is equivalent to $\max_{a>0}\{\lambda p\, a - (\phi/2)a^2\} > \tau_{\text{eff}}$. The objective is strictly concave in a with first-order condition $\lambda p - \phi a = 0$, so $a^* = \lambda p/\phi$ and the maximum value is $(\lambda p)^2/(2\phi)$. At the baseline calibration with $s_r = 0$, $\lambda p = 0.60 \times 4 = 2.4$ and $\tau_{\text{eff}} = \tau = 0.50$, hence

$$\frac{(\lambda p)^2}{2\phi} = \frac{2.4^2}{2 \times 5} = 0.576 > 0.50,$$

so the calibrated post-regulation tail is feasible.

Proof of Proposition 2.1. Differentiating (1) twice gives $\mathcal{L}'(K_T) = W'(K_\infty) - W'(K_T)$ and $\mathcal{L}''(K_T) = -W''(K_T) > 0$, so $\mathcal{L}$ is strictly convex with $\mathcal{L}(K_\infty) = \mathcal{L}'(K_\infty) = 0$. Two applications of the fundamental theorem of calculus and exchanging the order of integration deliver

$$\mathcal{L}(K_T) = \int_{K_\infty}^{K_T} (K_T - z)\, |W''(z)|\, \mathrm{d}z,$$

which is (3). Bounding the integrand below by $\underline{w}$ on the overhang yields the quadratic lower bound (4). The local quadratic (5) follows from a second-order Taylor expansion of W around K_∞ when $W \in C^3$. □

Proof of Proposition 2.2. Under $\mu(1-\lambda)p < \tau$, $D < \tau + (\rho + \delta)p$, and the steady-state formulae give $K_\infty < K^0 < K^*$. Hence $\mathcal{L}^{\text{stat}}(K) = (1-\lambda)p(K - K_\infty)$ on the relevant domain, and the ratio follows by cancellation. □

Proof of Proposition 2.4. At $\sigma = 0$, replacement investment $I = \delta K$ at the steady state lies in the investment region, so the FOC is

$$W'(K_\infty) = u'(c_\infty)(p + \phi\delta), \qquad c_\infty = \pi(K_\infty) - \tau_{\text{eff}} K_\infty - p\,\delta K_\infty - \tfrac{\phi}{2}\delta^2 K_\infty.$$

Differentiating the maximised HJB by the envelope theorem and evaluating at K_∞, with $\partial_K C|_{I=\delta K} = -\frac{\phi}{2}\delta^2$,

$$(\rho + \delta)\, W'(K_\infty) = u'(c_\infty)\big[\pi'(K_\infty) - \tau_{\text{eff}} + \tfrac{\phi}{2}\delta^2\big].$$

Substituting the FOC gives $(\rho+\delta)(p+\phi\delta) = \pi'(K_\infty) - \tau_{\text{eff}} + \frac{\phi}{2}\delta^2$, which rearranges to (22). Uniqueness follows from strict monotonicity of π' and the Inada condition. □

Remark B.2 (Stochastic correction). For $\sigma > 0$, the same envelope argument applied to the stochastic HJB (18) adds the term $\frac{1}{2}\sigma^2 K^2 W''(K)$ on the right of the deterministic FOC, so the zero-drift target K_∞^σ satisfies

$$\pi'(K_\infty^\sigma) \;=\; \tau_{\text{eff}} + (\rho+\delta)(p+\phi\delta) - \tfrac{1}{2}\phi\delta^2 + \sigma^2\,\Gamma(K_\infty^\sigma), \qquad \Gamma(K) \equiv -\frac{2K\,W''(K) + K^2\,W'''(K)}{2\,u'(c(K))}.$$

Γ is bounded and continuous in a neighbourhood of the deterministic root, so $K_\infty^\sigma = K_\infty + O(\sigma^2)$ by the implicit function theorem. At the calibrated $\sigma = 0.04$ the correction is of order 10^{-3}.

Proof of Lemma 2.7. The HJB (27) follows from a standard Poisson–diffusion derivation: the Bellman recursion over $[t, t+\mathrm{d}t]$ assigns probability $\mu\,\mathrm{d}t$ to a regime switch from V to W, Itô's formula handles the diffusion term, and taking $\mathrm{d}t \downarrow 0$ delivers the displayed HJB. The learning extension of Appendix A.1 replaces μ by the posterior mean $\hat{\mu}_t$ without changing the derivation. □

Proof of Proposition 2.8. Under $\gamma = 0$, $\phi = 0$, $\sigma = 0$, the pre-regulation HJB reads

$$(\rho+\mu)V(K) = \max_I \big\{\pi(K) + sK - pI + V'(K)(I-\delta K) + \mu W(K)\big\}.$$

The investment-region FOC gives $V'(K^*) = p$. Differentiating the maximised HJB by the envelope theorem and evaluating at K^*:

$$(\rho+\mu)p = \pi'(K^*) + s - \delta p + \mu W'(K^*).$$

The maintained region assumption gives $W'(K^*) = \lambda p$, and rearranging yields (28). □

Proof of Proposition 2.9. (i) At $\phi = 0$, the farmer sells $(K_T - \bar{K})$ instantaneously for $K_T > \bar{K}$, so $W_0(K_T) = \lambda p(K_T - \bar{K}) + W_0(\bar{K})$. Substituting into (1) with $W_0'(K_\infty) = p$ yields

$$\mathcal{L}|_{\phi=0}(K_T) = (1-\lambda)p\,(K_T - \bar{K}) + \Omega(\bar{K}, K_\infty), \qquad \Omega(\bar{K}, K_\infty) \equiv W_0(K_\infty) - W_0(\bar{K}) + p(\bar{K} - K_\infty).$$

Nonnegativity: on $[K_\infty, \bar{K}]$, $I = 0$ and W_0' lies between λp and p, so the mean-value theorem gives $W_0(\bar{K}) - W_0(K_\infty) \le p(\bar{K} - K_\infty)$, hence $\Omega \ge 0$ with equality iff $\lambda = 1$. The convergence rate $\eta = (-\rho + \sqrt{\rho^2 + 4|\pi''|K_\infty/\phi})/2 \to \infty$ as $\phi \to 0$, and uniform convergence $W_\phi \to W_0$ on compact subsets of $(0,\infty)$ follows from Fleming and Soner (2006).

(ii) At $\lambda = 1$, capital is perfectly reversible, $\bar{K} = K_\infty$, and $\mathcal{L}^{\text{stat}}(K_T) = 0$.

(iii) From (35), $\eta \to 0$ and $I^*(K) \to 0$ pointwise on compact sets, so capital adjusts only through depreciation. The pointwise limit $W_\infty(K) = AK^\alpha/(\rho+\alpha\delta) - \tau K/(\rho+\delta)$ is finite on compact sets bounded away from zero. However $K_\infty(\phi) \downarrow 0$ as $\phi \to \infty$, and $W_\infty'(K) \to +\infty$ as $K \downarrow 0$ by Inada, so the tangent term in the loss may diverge and no boundedness claim is made. □

Proof of Proposition 2.10. Under risk neutrality, the pre-regulation envelope condition with $\phi = \sigma = 0$ is $(\rho+\mu+\delta)V'(K^*) = \pi'(K^*)+s+\mu W'(\bar{K}^{\mathrm{RN}})$, with $V'(K^*) = p$ in the investment region and $W'(\bar{K}^{\mathrm{RN}}) = \lambda p$ at the post-liquidation entry point under $K^* > \bar{K}^{\mathrm{RN}}$. This yields $\pi'(K^*) = D - s$, and implicit differentiation gives $\partial K^*/\partial s = -1/\pi''(K^*) > 0$.

Consider the case $\gamma > 0$. The pre-regulation envelope becomes

$$(\rho + \mu + \delta)\frac{V'(K^*)}{u'(c^0(K^*))} = \pi'(K^*) + s + \mu\frac{W'(\bar{K}^{\mathrm{RN}})}{u'(c^0(K^*))},$$

with $V'(K^*) = u'(c^0(K^*)) \cdot p$ and $W'(\bar{K}^{\mathrm{RN}}) = u'(\tilde{c}^1) \cdot \lambda p$, $\tilde{c}^1 \equiv c^1(\bar{K}^{\mathrm{RN}})$. Defining

$$R(K^*, s, \gamma) \equiv \frac{u'(\tilde{c}^1)}{u'(c^0(K^*))} = \omega^\gamma, \qquad \omega \equiv \frac{c^0(K^*)}{\tilde{c}^1},$$

the feasibility condition (30) gives $\omega > 1$. Substituting,

$$\pi'(K^*) + s = (\rho + \delta)p + \mu(1 - \lambda R)\, p,$$

implicitly defines $K^*(s, \gamma)$ through $G(K^*, s, \gamma) \equiv \pi'(K^*)+s-(\rho+\delta)p-\mu(1-\lambda R)p = 0$. Crucially, the post-liquidation entry consumption $\tilde{c}^1 = c^1(\bar{K})$ depends on the policy parameters $(\tau, \lambda, p, \delta)$ but not on (K^*, s, γ), so the comparative-statics derivatives in s and K^* act on ω only through $c^0(K^*)$.

Part (i). The implicit function theorem gives $\partial K^*/\partial\gamma = -G_\gamma/G_{K^*}$. Now $G_\gamma = \mu\lambda p\, R \ln\omega$, which at $\gamma = 0$ is $\mu\lambda p \ln\omega > 0$ since $\omega > 1$, while $G_{K^*}|_{\gamma=0} = \pi''(K^*) < 0$, so $\partial K^*/\partial\gamma|_{\gamma=0} > 0$.

Part (ii). At $\gamma = 0$, $G_{K^*} = \pi''(K^*) < 0$ and continuity extends this to a neighbourhood of $\gamma = 0$. The total derivative of $\partial K^*/\partial s = -G_s/G_{K^*}$ in γ propagates through both the explicit γ-dependence of G and the equilibrium response $K^*_\gamma = -G_\gamma/G_{K^*}|_{\gamma=0} = \mu\lambda p\, \ln\omega/|\pi''(K^*)|$. Carrying the algebra at $\gamma = 0$ yields

$$\left.\frac{\partial^2 K^*}{\partial s\, \partial\gamma}\right|_{\gamma=0} = \frac{\mu\lambda p}{[\pi''(K^*)]^2}\left[|\pi''(K^*)|\,\frac{\partial \ln\omega}{\partial s} + \frac{\partial \ln\omega}{\partial K^*} + \frac{\pi'''(K^*)}{|\pi''(K^*)|}\,\ln\omega\right].$$

The third term arises from $G_{K^*K^*} = \pi'''(K^*)$ multiplied by K^*_γ. Each bracket term is strictly positive. Since $\tilde{c}^1$ is independent of (s, K^*), $\partial\ln\omega/\partial s = K^*/c^0(K^*) > 0$ and $\partial\ln\omega/\partial K^* = (\pi'(K^*) + s - \delta p)/c^0(K^*) = (D - \delta p)/c^0(K^*) > 0$ at the pre-regulation FOC, where the inequality uses $D = (\rho + \delta)p + \mu(1 - \lambda)p > \delta p$. Under Cobb–Douglas with $\alpha \in (0, 1)$, $\pi'''(K^*) = \alpha(\alpha-1)(\alpha-2)AK^{*,\alpha-3} > 0$ and $\ln\omega > 0$ by (30), so the third term is strictly positive. Hence the cross-partial is strictly positive. □

Remark B.3. At $\phi > 0$ the post-regulation value function is C^2 and consumption is the regular flow $c^1(K) = \pi(K) - \tau K - \tilde{p}(I^*)I^* - \frac{\phi}{2}(I^*)^2/K$ with $I^*(K) = K(q^*(K) - \lambda p)/\phi$. The implicit-function-theorem argument of Proposition 2.10 extends: the direct channel $G_\gamma = \mu\lambda p\, R \ln\omega > 0$ at $\gamma = 0$ is unchanged because it depends only on R, and G_{K^*} remains strictly negative by steady-state

stability, so the signs of $\partial K^*/\partial\gamma$ and $\partial^2 K^*/\partial s\,\partial\gamma$ extend from $\phi = 0$ to any bounded ϕ-interval by continuity. Table 11 confirms invariance numerically: $\mathcal{L}(K^*)$ moves by under 4% as ϕ varies by $\pm 50\%$ around $\phi = 5$.

Welfare ranking and zero-subsidy threshold (Section 4.4). The ranking $\mathcal{W}_{\text{FB}} \geq \mathcal{W}_{s^*} \geq \mathcal{W}_0$ follows because the first-best optimises over a weakly larger allocation set than any restricted constant-subsidy rule, and $s \equiv 0$ is feasible within the admissible class. As $\bar{s} \to D^-$, the fiscal cost $O(K^*)$ and stranding cost $O(K^{*2})$ dominate the $O(K^{*\alpha})$ production gain, so $\mathcal{W}_{\bar{s}} - \mathcal{W}_0 \to -\infty$. The intermediate value theorem then yields at least one crossing $\bar{s}_{\text{crit}} > 0$; uniqueness of the crossing and the reported value $\bar{s}_{\text{crit}} \approx 0.12$ are numerical, with $\Delta\mathcal{W}(s)$ single-crossing on the calibrated grid.

Proof of Lemma 3.1. Substitute $\pi'(K) = \alpha A K^{\alpha-1}$ into the steady-state conditions of Propositions 2.4 and 2.8 and invert. For (32), the full deterministic condition (Proposition 2.4) is $\pi'(K_\infty) = \tau_{\text{eff}} + (\rho+\delta)(p+\phi\delta) - \frac{1}{2}\phi\delta^2$. For (34), Proposition 2.8 (with $\gamma = 0$, $\phi = 0$, $\sigma = 0$) gives $\pi'(K^*) = D - s$. For (33), at $\phi = 0$ the inaction HJB on $[K_\infty, \bar{K}]$ reads $\rho W = \pi(K) - \tau K - \delta K\, W'$. Smooth pasting at the upper liquidation boundary gives $W'(\bar{K}) = \lambda p$. The classical solution to the deterministic free-boundary problem satisfies the high-contact condition $W''(\bar{K}) = 0$ (Dixit and Pindyck, 1994), imposed here as a property of the classical solution rather than a derived identity. Differentiating the inaction HJB in K and evaluating at $\bar{K}$ then yields $(\rho+\delta)\lambda p = \pi'(\bar{K}) - \tau$, so $\pi'(\bar{K}) = \tau + (\rho+\delta)\lambda p$ and (33) follows by inversion. □

Proof of Proposition 3.2. Under risk neutrality and $\sigma = 0$, the first-order condition for the post-regulation HJB gives $q = W'(K) = p + \phi\, I/K$, so $I = K(q-p)/\phi$. The capital law of motion becomes $\dot{K} = K(q-p)/\phi - \delta K$. The costate equation (from the current-value Hamiltonian) is

$$\dot{q} = (\rho+\delta)q - \pi'(K) + \tau - \frac{(q-p)^2}{2\phi}.$$

At steady state $q_\infty = p + \phi\delta$. Linearizing around (K_∞, q_∞) with $k \equiv K - K_\infty$, $\tilde{q} \equiv q - q_\infty$ gives the Jacobian

$$\begin{pmatrix} \dot{k} \\ \dot{\tilde{q}} \end{pmatrix} = \underbrace{\begin{pmatrix} 0 & K_\infty/\phi \\ |\pi''(K_\infty)| & \rho \end{pmatrix}}_{J} \begin{pmatrix} k \\ \tilde{q} \end{pmatrix}.$$

The characteristic polynomial $\lambda^2 - \rho\lambda - |\pi''(K_\infty)|K_\infty/\phi = 0$ has one positive and one negative root, $\lambda_\pm = \frac{1}{2}\left[\rho \pm \sqrt{\rho^2 + 4|\pi''|K_\infty/\phi}\right]$. The stable eigenvalue is $\eta = -\lambda_-$, which is (35). Along the saddle path, $k(t) = k(0)e^{-\eta t}$. □

Proof of Proposition 3.3. The drift $G : [0,\infty) \to \mathbb{R}$ is continuous and locally Lipschitz under the maintained regularity on π and u and on the optimal policy $I^*(K)$, so $\dot{K} = G(K)$ has a unique solution from each initial condition $K_0 \geq 0$. By Proposition 2.4, K_∞ is the unique zero of G on

$(0, \infty)$. Define the Lyapunov function $\mathcal{V}(K) \equiv \frac{1}{2}(K - K_\infty)^2$. Along any solution,

$$\dot{\mathcal{V}}(K_t) = (K_t - K_\infty)\, G(K_t) \leq -\underline{\eta}\,(K_t - K_\infty)^2 = -2\underline{\eta}\,\mathcal{V}(K_t),$$

where the inequality is (36). Gronwall's inequality gives $\mathcal{V}(K_t) \leq \mathcal{V}(K_0)\, e^{-2\underline{\eta} t}$, and taking square roots yields (37). □

Proof of Proposition A.1. The Gamma posterior under n arrival signals observed over horizon t is $\mu \mid (n, t) \sim \text{Gamma}(\alpha_0 + n, \beta_0 + t)$, so the posterior mean is $\hat{\mu}_{n,t} = (\alpha_0 + n)/(\beta_0 + t)$, whence $\partial \hat{\mu}_{n,t}/\partial n = 1/(\beta_0 + t) > 0$. Under the Cobb–Douglas steady-state formula,

$$K^*(\mu) = \left(\frac{\alpha A}{D(\mu) - s} \right)^{\frac{1}{1-\alpha}},$$

where $D(\mu)$ is affine and strictly increasing in μ. Therefore $K^*(\mu)$ is strictly decreasing in μ, so $\partial K^*/\partial n = (\partial K^*/\partial \hat{\mu}) \cdot (\partial \hat{\mu}/\partial n) < 0$. □

C Insurance and Biodiversity Extensions

C.1 Insurance Subsidy and Subsidy-Reform Complementarity

The insurance subsidy enters the pre-regulation FOC additively with CAP support (equation (42)); under Cobb–Douglas, the subsidised target is $K^*_{\text{eff}} = (\alpha A/(D - s_{\text{eff}}))^{1/(1-\alpha)}$ with $s_{\text{eff}} \equiv s_{\text{CAP}} + s_{\text{ins}}$.

Proposition C.1. *In the risk-neutral Cobb–Douglas benchmark ($\gamma = 0$, $\sigma = 0$, $\phi = 0$), $s_{\text{ins}} > 0$ strictly raises the subsidised target, the dynamic stranding loss, and the amplification multiplier: $K^*_{\text{eff}} > K^*$, $\mathcal{L}(K^*_{\text{eff}}) > \mathcal{L}(K^*)$, and $\mathcal{M}_{\text{eff}} \equiv \mathcal{L}(K^*_{\text{eff}})/\mathcal{L}(K^0) > \mathcal{M}$. The same monotone ranking holds on the calibrated HJB at $(\phi, \gamma) = (5, 2)$ (Table 9).*

Proof. The risk-neutral FOC (42) with $\pi'' < 0$ gives $K^*_{\text{eff}} > K^*$; the loss inequalities follow from monotonicity of $\mathcal{L}$ on $[K_\infty, \infty)$ and from strict convexity of $g(s) = \mathcal{L}_{\phi=0}(K^*(s))$ in s (the affine-composition argument of Proposition C.2 below). The calibrated extension is a numerical statement. □

Proposition C.2. *In the risk-neutral frictionless benchmark ($\gamma = 0$, $\sigma = 0$, $\phi = 0$) under Cobb–Douglas production, the reduction in stranding losses from removing the CAP subsidy is strictly larger when the insurance subsidy remains in place than when it has already been withdrawn, and symmetrically for removing the insurance subsidy:*

$$\Delta\mathcal{L}\big|_{s_{\text{CAP}} \to 0,\, s_{\text{ins}}} > \Delta\mathcal{L}\big|_{s_{\text{CAP}} \to 0,\, s_{\text{ins}} = 0}. \tag{50}$$

Equivalently, $\mathcal{L}(K^*(s_{\text{CAP}} + s_{\text{ins}}))$ is strictly supermodular in $(s_{\text{CAP}}, s_{\text{ins}})$ (subsidy-reform complementarity).

Proof. At $\phi = 0$, $\gamma = 0$, and $K^*(s) > \bar{K}$, Proposition 2.9(i) gives the closed form $\mathcal{L}_{\phi=0}(K^*(s)) = (1-\lambda)p\,(K^*(s) - \bar{K}) + \Omega(\bar{K}, K_\infty)$, affine in $K^*(s)$ above $\bar{K}$. The Cobb–Douglas target $K^*(s) = (\alpha A/(D-s))^{1/(1-\alpha)}$ is strictly increasing and strictly convex in s on $[0, D)$. The composite $g(s) \equiv \mathcal{L}_{\phi=0}(K^*(s))$ is therefore strictly convex in s as a positive affine transformation of a strictly convex function. Writing $s = s_{\text{CAP}} + s_{\text{ins}}$, strict convexity delivers

$$g(s_{\text{CAP}} + s_{\text{ins}}) + g(0) - g(s_{\text{CAP}}) - g(s_{\text{ins}}) \;>\; 0,$$

which rearranges to (50). The argument uses strict convexity of $K^*(s)$ rather than of $\mathcal{L}$, since the frictionless loss is affine in K above $\bar{K}$. □

The associated cross-partial of the loss in the subsidies is

$$\frac{\partial^2 \mathcal{L}(K^*(s_{\text{CAP}} + s_{\text{ins}}))}{\partial s_{\text{CAP}}\, \partial s_{\text{ins}}} \;>\; 0, \tag{51}$$

strictly positive in the frictionless benchmark; the calibrated HJB at $(\phi, \gamma) = (5, 2)$ preserves the sign numerically.

C.2 Two-Risk Biodiversity System

Four-regime HJB system. Index regimes by $(j, k) \in \{0, 1\}^2$ with $j = 1$ for carbon tax enacted and $k = 1$ for biodiversity regulation enacted. The absorbing regime is $(1, 1)$; the system is solved by backward induction. Regime $(1, 1)$ has combined charge $\tau + \tau_B$ and no subsidy:

$$\rho\, W^{11}(K) = \max_I \big\{ u\big(\pi(K) - (\tau + \tau_B)K - C(I, K)\big) + W^{11\prime}(K)(I - \delta K) + \tfrac{1}{2}\sigma^2 K^2 W^{11\prime\prime}(K) \big\}, \tag{52}$$

with frictionless steady state $K_\infty^{11,0} = (\alpha A/(\tau + \tau_B + (\rho+\delta)p))^{1/(1-\alpha)}$ in the $\phi = 0$ benchmark; under $\phi > 0$ the denominator carries the convex-adjustment premium $\phi\delta(\rho + \delta/2)$ as in Proposition 2.4. The frictionless target is the smallest of the four regime targets. Regime $(1, 0)$ (carbon tax enacted, biodiversity hazard outstanding):

$$(\rho + \hat{\nu})\, W^{10}(K) = \max_I \big\{ u\big(\pi(K) - \tau K - C(I, K)\big) + W^{10\prime}(K)(I - \delta K) + \tfrac{1}{2}\sigma^2 K^2 W^{10\prime\prime}(K) + \hat{\nu}\, W^{11}(K) \big\}. \tag{53}$$

Regime $(0, 1)$ symmetrically:

$$(\rho + \hat{\mu})\, W^{01}(K) = \max_I \big\{ u\big(\pi(K) - \tau_B K - C(I, K)\big) + W^{01\prime}(K)(I - \delta K) + \tfrac{1}{2}\sigma^2 K^2 W^{01\prime\prime}(K) + \hat{\mu}\, W^{11}(K) \big\}. \tag{54}$$

Regime $(0,0)$ is pre-regulation:

$$(\rho+\hat{\mu}+\hat{\nu})\,V(K) = \max_{I}\big\{u\big(\pi(K)+sK-C(I,K)\big)+V'(K)(I-\delta K) + \tfrac{1}{2}\sigma^2K^2V''(K)+\hat{\mu}\,W^{10}(K)+\hat{\nu}\,W^{01}(K)\big\}. \quad (55)$$

Both hazard rates enter the effective discount rate $\rho+\hat{\mu}+\hat{\nu}$; setting $\hat{\nu}=0$ recovers the single-risk model. For each regime $(j,k)\neq(0,0)$, the stranding loss

$$\mathcal{L}^{jk}(K) = W^{jk}(K^{jk}_\infty)+W^{jk\prime}(K^{jk}_\infty)(K-K^{jk}_\infty)-W^{jk}(K) \quad (56)$$

is zero at its regime-specific steady state and strictly positive for $K\neq K^{jk}_\infty$ by concavity of W^{jk}. The expected stranding loss at first policy arrival is

$$\bar{\mathcal{L}} = \frac{\hat{\mu}}{\hat{\mu}+\hat{\nu}}\,\mathcal{L}^{10}(K^{*,(2)})+\frac{\hat{\nu}}{\hat{\mu}+\hat{\nu}}\,\mathcal{L}^{01}(K^{*,(2)}). \quad (57)$$

The four regime targets are ordered $K^{11}_\infty < K^{10}_\infty < K^{01}_\infty < K^{*,(2)}$: the carbon charge is larger ($\tau=0.50$ versus $\tau_B=0.15$), so the carbon-only target sits below the biodiversity-only target.

Proposition C.3. *Under Cobb–Douglas production and frozen beliefs in the risk-neutral frictionless benchmark, the pre-regulation target under two risks satisfies*

$$\frac{K^*-K^{*,(2)}}{K^*} \;=\; 1-\Big(\tfrac{D-s}{D^{(2)}-s}\Big)^{1/(1-\alpha)}. \quad (58)$$

Proof. From $K^*(s)=(\alpha A/(D-s))^{1/(1-\alpha)}$ and $K^{*,(2)}(s)=(\alpha A/(D^{(2)}-s))^{1/(1-\alpha)}$, taking the ratio cancels αA and raises the denominator ratio to $1/(1-\alpha)$. □

At $\hat{\nu}=0.10$, $D^{(2)}=0.68$ against $D=0.52$, and $K^{*,(2)}=83.3$ LU against $K^*=207$ LU — a 73% increase in the net user cost $D-s$ amplified by the Cobb–Douglas exponent $1/(1-\alpha)=5/3$ to a 60% reduction in capital.

Charge-pair complementarity. The dynamic value function W^{11} has a free-boundary structure inherited from $\tilde{p}$ and is not available in closed form. The proposition below evaluates the cross-partial in a static fixed-capital comparator that holds K constant via replacement investment $I=\delta K$ regardless of optimality, with the comparator value $\widehat{W}^{11}(K)\equiv[AK^\alpha-\theta K]/\rho$, $\theta\equiv\tau+\tau_B+(\rho+\delta)p$. The subsidy-reform ranking used in the body is delivered separately by Lemma C.7; that result concerns the composite map from subsidies to inherited capital and then to expected loss, not the cross-partial of the dynamic loss in the regulatory charges.

Proposition C.4. *In the static fixed-capital comparator with Cobb–Douglas production and $\phi=\gamma=\sigma=0$, the comparator stranding loss*

$$\widehat{\mathcal{L}}^{11}(K;\tau,\tau_B) \;\equiv\; \widehat{W}^{11}(K^{11}_\infty)-\widehat{W}^{11}(K), \qquad \theta\equiv\tau+\tau_B+(\rho+\delta)p,$$

evaluated at the comparator steady state $K^{11}_{\infty} = (\alpha A/\theta)^{1/(1-\alpha)}$*, satisfies*

$$\frac{\partial^2 \widehat{\mathcal{L}}^{11}(K)}{\partial\tau\,\partial\tau_B} \;=\; \frac{1}{\rho(1-\alpha)}\,\frac{K^{11}_{\infty}}{\theta} \;>\; 0 \qquad \textit{for } K > K^{11}_{\infty}. \tag{59}$$

Proof. Holding K fixed via replacement investment $I = \delta K$ at flow $\pi(K) - \theta K + \delta p K - \delta p K = AK^{\alpha} - \theta K$, the comparator value is $\widehat{W}^{11}(K) = [AK^{\alpha} - \theta K]/\rho$. The comparator steady state $K^{11}_{\infty} = (\alpha A/\theta)^{1/(1-\alpha)}$ satisfies $\pi'(K^{11}_{\infty}) = \theta$ and $\widehat{W}^{11\prime}(K^{11}_{\infty}) = 0$. Differentiating $\widehat{\mathcal{L}}^{11} = \widehat{W}^{11}(K^{11}_{\infty}) - \widehat{W}^{11}(K)$ in θ at fixed K, the chain-rule term through $K^{11}_{\infty}(\theta)$ vanishes by $\widehat{W}^{11\prime}(K^{11}_{\infty}) = 0$, and the linear flow term $-\theta K$ contributes

$$\frac{\mathrm{d}\widehat{\mathcal{L}}^{11}}{\mathrm{d}\theta} = \frac{K - K^{11}_{\infty}}{\rho} > 0, \qquad \frac{\mathrm{d}^2\widehat{\mathcal{L}}^{11}}{\mathrm{d}\theta^2} = -\frac{1}{\rho}\,\frac{\mathrm{d}K^{11}_{\infty}}{\mathrm{d}\theta} = \frac{1}{\rho(1-\alpha)}\,\frac{K^{11}_{\infty}}{\theta} > 0,$$

where $\mathrm{d}K^{11}_{\infty}/\mathrm{d}\theta = -K^{11}_{\infty}/[(1-\alpha)\theta]$. Since $\partial\theta/\partial\tau = \partial\theta/\partial\tau_B = 1$, strict convexity in θ gives the cross-partial. □

A farm already bound by $\tau = 0.50$ bears a larger marginal comparator loss from an additional $\mathrm{d}\tau_B$ than a farm facing no regulation; the sign is increasing in α, so higher capital intensity amplifies the interaction. The comparator is not the dynamic value function: $I = \delta K$ above K^{11}_{∞} is sub-optimal in the dynamic problem, where $\phi = 0$ delivers the free-boundary structure of Proposition 2.9(i). The dynamic cross-partial is reported numerically in Figure 6 and matches the comparator sign on a right neighbourhood of K^{11}_{∞} (Proposition C.5).

Decomposition at $(\phi, \gamma) > 0$. Away from the frictionless benchmark, the numerical cross-partial of the dynamic loss decomposes additively into three diagnostic components,

$$\frac{\partial^2 \mathcal{L}^{11}(K;\phi,\gamma)}{\partial\tau\,\partial\tau_B} \;=\; A(\theta_0;\alpha) + B_{\phi}(K;\theta_0,\alpha) + C_{\gamma}(\theta_0;\alpha), \tag{60}$$

with $\theta_0 \equiv \tau + \tau_B$. The envelope term $A(\theta_0;\alpha) = K^{11}_{\infty}/[\rho(1-\alpha)\theta]$ is strictly positive and corresponds to the frictionless benchmark of Proposition C.4; at the calibration it evaluates to ≈ 672 in utility units in the $\phi = 0$ analytical limit. The overhang term B_{ϕ} vanishes at $K = K^{11}_{\infty}$, is zero for $\phi = 0$, and is strictly negative for sufficiently large overhang, because convex adjustment penalises a combined charge that forces large disinvestment more than two charges applied separately. The prudence term C_{γ} is approximately independent of K, zero at $\gamma = 0$, and strictly negative for $\gamma > 0$: a joint charge depresses the post-regulation consumption floor c_{∞}, and the cross-product $u''(c_{\infty})\,(\partial c_{\infty}/\partial\tau)(\partial c_{\infty}/\partial\tau_B)$ contributes negatively with magnitude scaling linearly in γ. Figure 6 plots the cross-partial across (K_T, ϕ) under $u(c) = c$ and under CRRA with $\gamma = 2$.

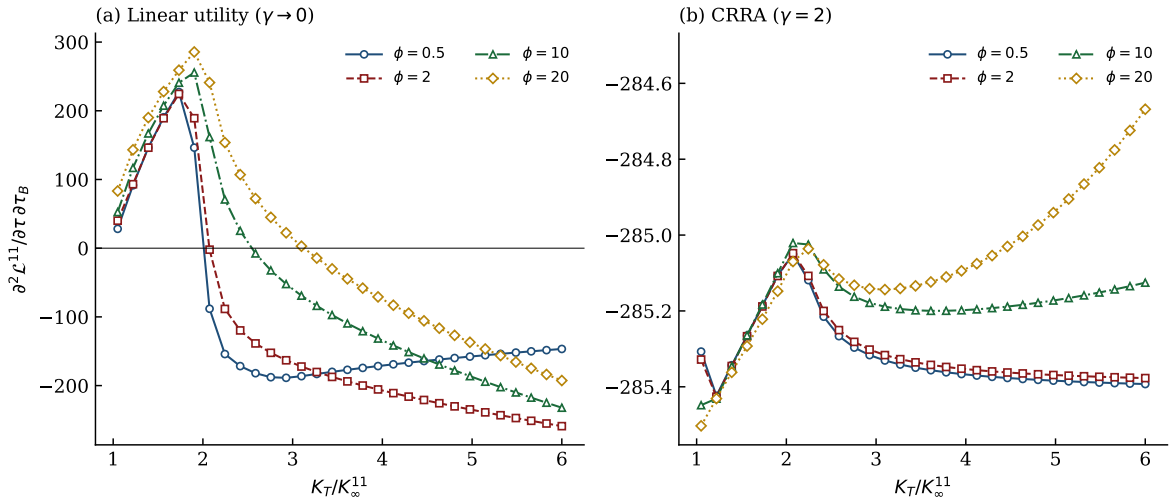

Figure 6: Cross-partial $\partial^2 \mathcal{L}^{11} / \partial \tau \, \partial \tau_B$ as a function of K_T / K_∞^{11} for four values of ϕ, at $\theta_0 = 0.65$. Panel (a): linear utility. Panel (b): CRRA with $\gamma = 2$; the y-axis is zoomed to the data range to expose the small ϕ-spread, which is of order 10^{-1} relative to a level of order 10^2 set by the prudence term.

Panel (a) traces the overhang-driven sign flip: under linear utility the cross-partial is positive on a neighbourhood of K_∞^{11}, peaks at ≈ 290 around $K_T / K_\infty^{11} \approx 1.8$, and reverses beyond a threshold $\bar{K}(\phi)$ that shifts right as ϕ rises. Panel (b) shows that CRRA at the calibrated $\gamma = 2$ shifts the curve uniformly below zero to a band near -285; the zoomed y-axis exposes a small ϕ-spread of order 10^{-1} — the $\phi = 20$ curve lifts slightly above the tighter cluster formed by $\phi \in \{0.5, 2, 10\}$ — confirming that B_ϕ and the ϕ-response of C_γ are small relative to the level of C_γ at $\gamma = 2$. The prudence term accounts for the K-independent downward shift from panel (a) to panel (b); the overhang term accounts for the ϕ-dependent K-slope visible only in panel (a).

Proposition C.5. *Under Cobb–Douglas production, $u(c) = c$, $\sigma = 0$, and $\phi \geq 0$, for every compact interior set $\mathcal{D} \subset \mathbb{R}_+^2 \times (0,1)$ of parameters (ϕ, θ_0, α) there exists $\bar{K}(\phi, \theta_0, \alpha) > K_\infty^{11}$ such that*

$$\frac{\partial^2 \mathcal{L}^{11}(K; \phi, \gamma = 0)}{\partial \tau \, \partial \tau_B} > 0 \qquad \text{for all } K \in (K_\infty^{11}, \bar{K}]. \tag{61}$$

Proof. At $K = K_\infty^{11}$ the overhang term $B_\phi(K_\infty^{11}; \theta_0, \alpha) = 0$ and the prudence term C_γ vanishes at $\gamma = 0$, so the cross-partial equals $A(\theta_0; \alpha) > 0$ by Proposition C.4. Joint continuity of $\mathcal{L}^{11}$ in K and its second derivatives in (τ, τ_B) on the interior (K_∞^{11}, ∞) delivers a right neighbourhood on which the strict inequality persists. □

Remark C.6. At the baseline calibration $(\phi, \theta_0, \alpha) = (5, 0.65, 0.40)$, numerical evaluation of the HJB system yields $\bar{K} \approx 2.2 \, K_\infty^{11}$ under linear utility. The calibrated $K_T = 83.3$ LU exceeds this threshold (panel (a) of Figure 6).

CRRA interaction. At the calibrated $\gamma = 2$, the cross-partial $\partial^2 \mathcal{L}^{11} / \partial \tau \, \partial \tau_B$ is negative for all $K > K_\infty^{11}$, flat in the overhang to leading order (panel (b) of Figure 6). The mechanism runs

through prudence at the post-regulation consumption floor: a joint charge $\theta_0 = \tau + \tau_B$ depresses c_∞, and the contribution

$$u''(c_\infty) \cdot \frac{\partial c_\infty}{\partial \tau} \cdot \frac{\partial c_\infty}{\partial \tau_B}$$

is negative because $u''(c_\infty) = -\gamma c_\infty^{-\gamma-1} < 0$ while both marginal consumption responses are negative. The magnitude scales linearly in γ and is approximately independent of K and ϕ, so the curves in panel (b) collapse onto a single line and shift rigidly below the $\gamma = 0$ curves of panel (a). At the baseline this downward shift is of order -285 in utility units (≈ -15 EUR '000 via the annuity $u'(c_\infty)/\rho$), exceeding the numerical peak of $A + B_\phi \approx 290$ reached in panel (a), and therefore driving the cross-partial strictly negative across the plotted range of (K_T, ϕ).

The reform ranking of Lemma C.7 is insensitive to the sign of this cross-partial. The lemma runs through the composite $g(s) \equiv \bar{\mathcal{L}}(K^{*,(2)}(s))$. In the frictionless benchmark, strict convexity of g comes from strict convexity of $K^{*,(2)}(s)$ in s composed with affine maps $\mathcal{L}^{jk}_{\phi=0}$ above $\bar{K}^{jk}$; in the calibrated HJB, strict convexity of g is verified numerically. Either way, the ranking is preserved regardless of the sign of $\partial^2 \mathcal{L}^{11} / \partial\tau \, \partial\tau_B$:

Lemma C.7. *Define $g(s) \equiv \bar{\mathcal{L}}(K^{*,(2)}(s))$. In the deterministic risk-neutral frictionless benchmark ($\gamma = 0$, $\sigma = 0$, $\phi = 0$) under Cobb–Douglas production and frozen beliefs, $g(s_{\text{CAP}} + s_{\text{bio}})$ is strictly supermodular in $(s_{\text{CAP}}, s_{\text{bio}})$. The same ranking holds on the calibrated HJB at $(\phi, \gamma) = (5, 2)$, evaluated numerically against the four-regime system (52)–(55); an analytical extension to all $(\phi, \gamma) \geq 0$ is not established.*

Proof. At $\gamma = 0$, $\phi = 0$, $\sigma = 0$, and $K^{*,(2)}(s) > \bar{K}^{jk}$ for $jk \in \{10, 01\}$, Proposition 2.9(i) applied at each regime gives $\mathcal{L}^{jk}_{\phi=0}(K)$ affine in K above $\bar{K}^{jk}$. The closed form $K^{*,(2)}(s) = (\alpha A/(D^{(2)} - s))^{1/(1-\alpha)}$ is strictly convex in s on $[0, D^{(2)})$. Hence $g(s) \equiv \bar{\mathcal{L}}(K^{*,(2)}(s))$ is strictly convex in s as a positive affine transformation of a strictly convex function, and the mixed difference $g(s_{\text{CAP}} + s_{\text{bio}}) + g(0) - g(s_{\text{CAP}}) - g(s_{\text{bio}}) > 0$ delivers supermodularity. The argument routes through strict convexity of $K^{*,(2)}$ rather than of $\bar{\mathcal{L}}$, since $\mathcal{L}^{jk}_{\phi=0}$ is affine in K. At $(\phi, \gamma) > 0$, $K^{*,(2)}(s)$ is no longer given by the Cobb–Douglas closed form, and the analytical argument does not extend; numerical verification on the calibrated grid is reported as a supporting result. □

Calibration. All parameters except those in Table 15 retain their Table 4 values. The biodiversity charge $\tau_B = 0.15$ EUR '000/LU/yr is bracketed by England's Biodiversity Net Gain statutory units (annualising to roughly €180–€400/ha), CAP eco-scheme withdrawal for non-compliance (≈€120/ha), and Denmark's Green Tripartite opportunity cost (€100–€240/LU/yr). Jacobsen et al. (2019) report Danish ammonia-regulation compliance costs near Natura 2000 sites in the range €150–€200/LU/yr (scaled from per-farm figures up to roughly €30,000/farm/yr at 150–200-LU herds), within the τ_B range. The arrival rate $\hat{\nu} = 0.10$ has two anchors. The calendar midpoint of announcement (2020) and enforcement (2030) of the Nature Restoration Regulation fixes a decadal transition frequency. Independently, Giglio et al. (2025b) report a 10-K transition-risk score of 0.437 for GICS sector 3020 (Food, Beverage & Tobacco), among the highest cross-sectorally and

consistent with a market-implied arrival rate in the 0.08–0.15 range at a ten-year horizon; the baseline sits at the lower end of that band.

Table 15: Biodiversity-regulation parameters

Parameter	Symbol	Value	Source
Biodiversity charge	τ_B	0.15	BNG / eco-scheme / Green Tripartite
Arrival rate	$\hat{\nu}$	0.10	Pre-signal Poisson
Noncompliance subsidy	s_{bio}	0.13	$\tau_B^{\text{eff}} - \tau_B^{\text{actual}}$

Table 16 compares single- and two-risk steady states. The biodiversity risk adds €160/LU/yr to the user cost; the terminal targets are ordered joint < carbon-only < biodiversity-only, reflecting $\tau > \tau_B$.

Table 16: Single-risk versus two-risk steady states

	Single risk ($\hat{\nu} = 0$)	Two risks ($\hat{\nu} = 0.10$)	Change
User cost D (EUR '000/LU/yr)	0.520	0.680	+30.8%
Net user cost $D - s$	0.220	0.380	+72.7%
Pre-reg. target K^* (LU)	207.1	83.3	−59.8%
No-subsidy target K^0 (LU)	49.4	31.6	−36.1%
Terminal carbon-only target (LU)	21.3	21.3	0
Terminal biodiversity-only target (LU)	—	51.0	—
Terminal joint target (LU)	—	16.3	—

Notes: The terminal targets are absorbing-regime zero-drift benchmarks. The four-regime HJB targets K_∞^{jk} from (52)–(55) carry continuation-value terms $\hat{\nu}W^{11}(K)$ and $\hat{\mu}W^{11}(K)$ and are computed numerically. The table reports the absorbing-regime benchmarks. $D^{(2)} = 0.36 + 0.32 = 0.68$.

Table 17 reports capital overhangs at the pre-regulation target. Under two risks the overhang is smaller because the farmer anticipates both shocks and accumulates less. Total physical overhang under simultaneous and sequential arrival is the same (67.0 LU in both cases); welfare consequences differ because convex adjustment penalises concentration of 67.0 LU of disinvestment at a single instant more heavily than the same total spread across two dates.

Table 17: Capital overhangs under two policy risks

Arrival scenario	Prob.	K at arrival	Overhang (LU)
Carbon tax first	0.50	83.3	62.0
Biodiversity reg. first	0.50	83.3	32.3
Both simultaneous	—	83.3	67.0
Single-risk baseline ($\hat{\nu} = 0$, $K^* = 207.1$)			185.8

Notes: Overhang $= K^{*,(2)} - K_{\infty}^{jk}$.

Learning and signals. The Gamma–Poisson conjugate of Appendix A.1 carries over to each risk separately. Five European events between 2020 and 2025 raise $\hat{\nu}$: the EU Biodiversity Strategy (May 2020), the draft Nature Restoration Regulation (June 2022), the CAP eco-scheme launch (January 2023), the Regulation's entry into force (August 2024), and the Danish Green Tripartite (June 2024). Under a Gamma$(2, 20)$ prior, these signals push $\hat{\nu}$ from 0.10 to approximately 0.28 by end-2024 — a trajectory comparable to the carbon-tax posterior in Table 14.

When biodiversity and carbon signals arrive bundled, as with the Green Tripartite, the posterior means jump simultaneously; the additive entry of $\hat{\mu}$ and $\hat{\nu}$ in equation (43) avoids double-counting since the two stranding premia $\hat{\mu}(1-\lambda)p$ and $\hat{\nu}(1-\lambda)p$ enter $D^{(2)}$ as separate linear contributions. Since $K^{*,(2)}$ depends only on the sum $\hat{\mu} + \hat{\nu}$, the cumulative target change is identical under bundled and sequential announcements of equal aggregate magnitude, but the bundled case forces a single large discrete contraction whose welfare cost exceeds the spread-out case because of convex adjustment. Giglio et al. (2025b,a) show biodiversity risk is already priced in equity and CDS markets; for GICS sector 3020 (Food, Beverage & Tobacco) the 10-K transition-risk score is 0.437 and the physical-risk score 0.584 — both among the highest, consistent with $\hat{\nu}$ in the 0.10–0.20 range.

D Cross-Country Portability

Applying the Danish calibration to four other EU jurisdictions probes the portability of the mechanism under heterogeneous arrival rates and subsidy levels. Each row applies a Danish-calibrated carbon tax ($\tau = 0.50$) and Danish-calibrated structural parameters, holding the mechanism fixed while varying (A_j, s_j, μ_j).

Calibration. Inverting the steady-state condition gives

$$A_j \;=\; \frac{D_j - s_j}{\alpha}\left(K^*_{\text{obs},j}\right)^{1-\alpha},$$

with $D_j = (\rho + \delta)p + \mu_j(1-\lambda)p$ the country-specific user cost; s_j matches average CAP direct payments per livestock unit, and all remaining structural parameters are held at Danish values. Arrival rates are assumed rather than estimated: Denmark ($\mu = 0.10$) has legislated a CO_2e tax

from 2030; the Netherlands ($\mu = 0.12$) faces the *Stikstofcrisis* with mandatory herd reductions and EUR 1.47 billion in buyout programmes; Ireland ($\mu = 0.08$) has committed to a 25% agricultural-emissions reduction by 2030; Germany ($\mu = 0.05$) has sectoral targets under the *Klimaschutzgesetz* but no livestock-specific levy; France ($\mu = 0.03$) has no agriculture-specific carbon instrument under active consideration. Table 19 reports amplification under ±50% perturbations.

Table 18: Cross-country stranding exposure under a uniform Danish-scale shock

Country	A	s	μ **(yr^{-1})**	K^*_{obs} **(LU)**	K^* **(LU)**	K_∞ **(LU)**	$\mathcal{L}$	**CV (EUR)**	$\mathcal{M}$
Denmark	13.49	0.30	0.10	207	207.0	21.3	0.654	25,042	13.2
France†	2.64	0.35	0.03	126	126.0	1.4	122.641	20,446	61.9
Netherlands	19.74	0.15	0.12	143	143.0	40.3	0.072	9,760	3.6
Germany	8.81	0.25	0.05	130	130.0	10.5	1.818	16,844	9.0
Ireland	14.32	0.20	0.08	146	146.0	23.6	0.316	14,766	5.3

Notes: $\mathcal{M} = \mathcal{L}(K^*(s))/\mathcal{L}(K^*(0))$ at a uniform Danish-scale $\tau = 0.50$. Herd data: DK from Danish Agriculture and Food Council (2019); others from Eurostat `ef_lus_main` (2022). † The France row imposes a Danish-scale tax on a low-TFP environment: $A_{\text{FR}} = 2.64$ inverts from a 126-LU observed herd, which forces $K^{\text{FR}}_\infty \approx 1.4$ LU at $\tau = 0.50$. A French-specific exercise would recalibrate emissions intensity, output prices, and the mapping from cattle headcount to productive capital.

Low μ generates larger stranding exposure at a given τ: farmers accumulate toward a subsidy-inflated target without the user-cost discipline imposed by an anticipated tax. At $\tau = 0.50$ and $A_{\text{FR}} = 2.64$, K^{FR}_∞ falls below two cows and amplification is an order of magnitude larger than in Denmark. The Netherlands compresses the overhang through lower subsidies, higher μ driven by the nitrogen crisis, and high productivity.

Table 19: Sensitivity of amplification multiplier to arrival-rate assumptions

Country	$\mathcal{M}$ ($\mu_j \times 0.5$)	$\mathcal{M}$ (baseline)	$\mathcal{M}$ ($\mu_j \times 1.5$)
Denmark	17.7	13.2	13.0
Netherlands	3.6	3.6	4.4
Ireland	5.8	5.3	5.4
Germany	10.7	9.0	8.1
France	130.9	61.9	39.9

Notes: μ_j perturbed ±50%; other parameters at baseline. Values rescaled to the HJB-solved baseline in Table 18.

Insurance across countries. Table 20 applies the insurance calibration of Section 5.1 to the five-country sample using the calibrated A_j from Table 18. The Dutch Brede Weersverzekering carries a statutory ceiling of 63.7% with realised 2024–2025 subsidies of 46–57% ($\zeta = 0.50$). The

German Mehrgefahrenversicherung is co-financed at up to 50% by the federal states ($\zeta = 0.50$). Pass-through ψ is not estimated in the public literature; $\psi = 0.35$ for NL and $\psi = 0.40$ for DE because the Dutch product covers arable crops rather than livestock and the German product reaches specialist dairy farms only partially. Expected damage rates are country-specific: 0.050 for France (CCR 2023 dairy losses), 0.080 for the Netherlands (higher grassland yield volatility), 0.060 for Germany (BMEL *Agrarbericht* 2023). The France value $s_{\text{ins}} = 0.030$ here slightly exceeds the Danish calibration 0.027 in Table 4 because this exercise uses the 2023 CCR payout base rather than the 2018–2023 average.

Table 20: Insurance amplification across countries

Country	s_{CAP}	s_{ins}	s_{eff}	K^*_{eff} (LU)	$\mathcal{M}_{\text{eff}}$
Denmark	0.300	0.000	0.300	207.1	13.2
France	0.350	0.030	0.380	424.1	216.0
Netherlands	0.150	0.014	0.164	151.7	4.1
Germany	0.250	0.012	0.262	144.9	10.3
Ireland	0.200	0.000	0.200	146.0	5.3

Notes: s_{CAP}, μ, and A from Table 18. DK and IE have no state-subsidised crop insurance ($s_{\text{ins}} = 0$). The France entry uses the inverted $A_{\text{FR}} = 2.64$ from Table 18.

France records the largest amplification in the sample under the combination of high CAP payments and the insurance subsidy. The Dutch product covers arable crops, limiting pass-through to dairy capital; Denmark and Ireland have no state-subsidised crop insurance.

E Robustness Checks

Risk aversion. For $\gamma \in \{0.5, 1, 2, 4, 6\}$, the productivity scale $A(\gamma)$ is recalibrated to match $K^* = 207.1$ LU. Recalibration isolates the curvature effect on welfare from the level effect on K^*: at fixed A, Proposition 2.10 delivers $\partial K^*/\partial\gamma > 0$ and the calibrated solution puts the increase at 8% to 25% across $\gamma \in [1, 4]$. The consumption-gap complementarity $\partial^2 K^*/\partial s\,\partial\gamma > 0$ operates through the level of K^* at fixed A and is suppressed by construction in Table 21. The subsidised CV ranges over EUR 21,792–28,153 (29% spread); $\mathcal{M}$ falls monotonically from 15.2 to 10.2 because higher risk aversion flattens the utility-unit loss function more at K^* than at K^0.

Table 21: Robustness to risk aversion

	$\gamma = 0.5$	$\gamma = 1$	$\gamma = 2$	$\gamma = 4$	$\gamma = 6$
K^* (LU)	207.1	207.1	207.1	207.1	207.1
CV at K^* (EUR)	21,792	23,227	25,045	26,989	28,153
CV at K^0 (EUR)	1,435	1,606	1,901	2,394	2,761
$\mathcal{M}$	15.2	14.5	13.2	11.3	10.2

Notes: $A(\gamma)$ is recalibrated at each γ to match $K^* = 207.1$ LU; all other parameters at Table 4 values. CV is the linearised money-metric of equation (39).

Other checks. The Gomes (2001) output-scaled adjustment cost $C^G(I, K) = pI + \frac{\phi_G}{2} I^2/Y$ with $Y = AK^\alpha$ and $\phi_G = \phi A(K^*)^{\alpha-1} \approx 2.75$ (matched at the pre-regulation steady state) lowers $\mathcal{M}$ from 13.2 to 13.0 and the baseline CV from EUR 25,045 to EUR 23,680. CES production $\pi(K) = A[\alpha K^{(\varepsilon-1)/\varepsilon} + (1-\alpha)]^{\varepsilon/(\varepsilon-1)}$ over $\varepsilon \in [0.5, 2.0]$ shifts $\mathcal{L}$ by $\pm 12\%$: gross complements ($\varepsilon < 1$) steepen the marginal-product curve and compress the overhang, gross substitutes ($\varepsilon > 1$) flatten it and expand the loss. A deterministic time-varying hazard $\mu(t) = \mu_0 + \mu_1 t$ calibrated to match the constant-μ 30-year arrival probability brackets the baseline at -6% (front-loaded) to $+8\%$ (back-loaded). A two-state regime-switching hazard at $(\mu_L, \mu_H) = (0.04, 0.16)$ with transition intensity $\eta = 0.1$ and ergodic mean $\mu = 0.10$ yields an ergodic-average loss within 3% of the baseline.

F Numerical Method

This appendix gives the discretisation, the implicit linear system, the boundary treatment, and converged value-function levels for replication.

Finite differences and upwind scheme. At each iteration n, $W'(K_i)$ is approximated by forward and backward differences,

$$W'_{i,F} = \frac{W^n_{i+1} - W^n_i}{\Delta K}, \qquad W'_{i,B} = \frac{W^n_i - W^n_{i-1}}{\Delta K},$$

on the uniform grid $\{K_1, \ldots, K_N\}$ with spacing $\Delta K = (K_N - K_1)/(N-1)$. The upwind selection follows the sign of the drift:

$$W'_i = \begin{cases} W'_{i,F} & \text{if } I^*_i - \delta K_i > 0, \\ W'_{i,B} & \text{if } I^*_i - \delta K_i < 0, \\ \frac{1}{2}(W'_{i,F} + W'_{i,B}) & \text{otherwise.} \end{cases}$$

Investment optimisation. The optimal $I^*(K_i)$ is computed by vectorised grid search over 150 candidate values for positive investment and 150 for negative; the candidate set always includes $I = 0$ exactly, so the inaction region is selected directly rather than approximated by small positive

or negative investment, and candidates that violate $c_i > 0$ are discarded before evaluation.

Implicit time stepping. Backward Euler advances the value function:

$$\frac{W_i^{n+1} - W_i^n}{\Delta t} + \rho W_i^{n+1} = u(c_i^n) + \mathcal{A}^n W_i^{n+1}, \tag{62}$$

which in matrix form is $[(\Delta t)^{-1}\mathbf{I} + \rho\mathbf{I} - \mathbf{A}^n]\mathbf{W}^{n+1} = (\Delta t)^{-1}\mathbf{W}^n + \mathbf{u}^n$, solved by sparse direct factorisation. Implicit stepping permits $\Delta t = 1$ year without CFL restriction.

Boundary conditions. Natural zero-curvature: $W'(K_1) = W'(K_2)$ and $W'(K_N) = W'(K_{N-1})$, equivalent to $W''(K_1) = W''(K_N) = 0$.

Solution procedure. The post-regulation problem is solved first to obtain W; the pre-regulation problem then takes W as terminal value. Converged value functions are interpolated by monotone PCHIP. Numerical value-function levels are reported in the replication package; Table 8 provides the welfare-relevant money-metric summaries used in the body.